First occurrence of musk ox *Ovibos moschatus* in the Late Pleistocene (MIS 3) record from NW Iberia: Paleobiogeographic and paleoenvironmental implications

Diego J. Álvarez-Lao [a,*], Daniel Ballesteros [b], Florent Rivals [c,d,e], Adrián Álvarez-Vena [a], Pablo Valenzuela [f], Montserrat Jiménez-Sánchez [a]

[a] *Departamento de Geología, Universidad de Oviedo, C/ Jesús Arias de Velasco s/n., E-33005, Oviedo, Spain*
[b] *UMR 6266 IDEES, Université de Rouen-Normandie/CNRS, Mont Saint-Aignan CEDEX, France*
[c] *Institució Catalana de Recerca i Estudis Avançats (ICREA), Barcelona, Spain*
[d] *Institut Català de Paleoecologia Humana i Evolució Social (IPHES), Campus Sescelades URV (Edifici W3), 43007, Tarragona, Spain*
[e] *Universitat Rovira i Virgili (URV), Area de Prehistoria, Avinguda de Catalunya 35, 43002, Tarragona, Spain*
[f] *TRAGSATEC S.A, c/ Julián Camarillo 6B, 28037, Madrid, Spain*

ARTICLE INFO

ABSTRACT

A remarkable musk ox (*Ovibos moschatus*) assemblage was recovered at Cowshead Cave (Picos de Europa Mountains, NW Spain). This find is of special paleobiogeographic relevance since it involves the first occurrence of this species in NW Iberia and extends the boundary of its Eurasian distribution range to the SW. Fossils correspond to at least two individuals: one young male about 20 months old, which includes an extraordinarily well-preserved skull, and one subadult of about 38–44 months. The bone deposit, dated to 34.9 ± 0.4 cal ka BP (MIS 3), accumulated in a karst cave that acted as a natural trap, agreeing with the geomorphology and the good preservation of the remains. Considering that musk ox skulls of young individuals are extremely rare in the Pleistocene record, the detailed comparative study of the skull here presented provides new and relevant information. The skull from Cowshead is larger than modern specimens of similar individual age from Greenland; additionally, some remarkable morphological peculiarities in skull and teeth were identified. One metacarpal of the subadult individual was compared to recent and Pleistocene specimens and was among the largest in the entire sample. Significant differences in morphology and size between fossil and recent metacarpals were detected. Teeth microwear analysis suggests a browsing diet based on twigs and leaves at the time of death, which is consistent with a winter diet. The cold and arid environment inferred from the presence of musk ox is consistent with the paleontological record, since cold-adapted mammals occurred at other contemporary assemblages from NW Iberia.

© 2020

1. Introduction

The musk ox *Ovibos moschatus* (Zimmermann, 1780) is one of the key species of the mammoth fauna (Vereschagin and Baryshnikov, 1982) or *Mammuthus-Coelodonta* faunal complex (Kahlke, 1999, 2014), a mammal community composed of cold-adapted species which lived throughout the middle and high latitudes of Eurasia and North America during the Late Pleistocene. During the coldest episodes, this faunal complex expanded to the southernmost regions of Europe reaching the Iberian Peninsula, which constituted its SW boundary: finds of woolly mammoth (*Mammuthus primigenius*), woolly rhinoceros (*Coelodonta antiquitatis*) and reindeer (*Rangifer tarandus*), although scarce, are reported in a number of Iberian sites, especially from the North (Cantabrian Region and Catalonia; Altuna, 1996; García

and Arsuaga, 2003; Álvarez-Lao et al., 2009, 2017; Álvarez-Lao and García, 2010, 2011a, 2011b, 2012). Iberian occurrences of these species are relatively more frequent during the Marine Isotope Stage (MIS) 3, an episode characterized by numerous and abrupt climate changes, from extreme cold to temperate conditions (Barron and Pollard, 2002; van Andel, 2002).

This mammal community was closely related to the steppe-tundra or mammoth steppe (Guthrie, 1982), an herbaceous ecosystem distinctive of the Quaternary glacial periods. At the end of the Pleistocene the steppe-tundra vanished and, consequently, the mammoth fauna also disappeared as a community: some of these species (for example, woolly mammoth and woolly rhinoceros) became extinct, others (such as reindeer and musk ox) moved northward to arctic refuges, and some others (like the saiga antelope *Saiga tatarica*) migrated to the central Asian steppe.

The musk ox became extinct at most of its Pleistocene geographical range, including all Eurasia. Evidences point to this extinction being related to environmental change (mainly climatic warming) and not

* Corresponding author.
  E-mail address: dalao@geol.uniovi.es (D.J. Álvarez-Lao).

to anthropogenic causes (Campos et al., 2010; Lorenzen et al., 2011). It still survives in Northern Canada and Greenland; additionally, several populations were successfully re-introduced in Alaska, Siberia and Scandinavia (Tener, 1965; Lent, 1988). Its maximum spread was reached during the Late Pleistocene coldest episodes (Kahlke, 2014), expanding through extensive areas of Eurasia, including the Iberian Peninsula. However, Iberian occurrences of this species are extremely rare, with only two findings reported so far, both from Catalonia, NE Iberia (Estévez Escalera, 1978; Álvarez-Lao and García, 2010).

Pleistocene *Ovibos* were often ascribed to more than one species: for instance, *O. pallantis* Smith, 1827, a fossil species defined on the basis of anatomic differences between Pleistocene and modern populations, was accepted by different authors (e.g. Khan, 1966; Sher, 1971; Tikhonov, 1998). Today, however, DNA analyses indicate that both fossil and modern populations correspond to the single species *O. moschatus*, while it is accepted that genetic diversity was much higher during the Pleistocene than it is today (MacPhee et al., 2005; Campos et al., 2010).

In 1986, the Lancaster University Speleological Society and the South Wales Caving Club, during a speleological exploration of a cave near Tresviso (Cantabria; Fig. 1), discovered a bone assemblage comprising an almost complete skull, which was initially interpreted as remains of cows (Newman and Walker, 1987). The cavity, which is more than 3 km long, was named Cowshead Cave after this discovery and was inventoried as T516 by the Tresviso Caves Project (www.tresvisocaves.info). In July 2018, a team from the Universidad de Oviedo composed by paleontologists, geomorphologists and speleologists, recovered this bone assemblage from the Cowshead Cave, within the framework of a research project performed in the caves of the Picos de Europa National Park. The detailed study of these fossils, here presented, allowed their ascription to musk ox (*O. moschatus*). This discovery is of high relevance, especially from a paleobiogeographic perspective, since it constitutes the first occurrence of *O. moschatus* from NW Iberia, and delimits the SW border of the Eurasian distribution of this species. In addition, the good preservation of these fossils allowed the development of a detailed anatomical comparative study.

The main goals of this work are: (1) to present and describe the paleontological site from a geomorphologic perspective to understand the origin of the fossil accumulation, (2) to provide a detailed comparative study of the fossils in order to identify similarities or differences with other modern and fossil populations, (3) to infer the dietary traits based on teeth microwear in order to assess the available plant resources and, thus, the vegetal landscape, and (4) to discuss the paleobiogeographic and (5) paleoenvironmental implications of this relevant discovery.

2. Setting

The entrance of Cowshead Cave (843 m altitude) is located in the southwestern end of the Sobra Valley (Fig. 1), in the northern part of the Eastern Massif of the Picos de Europa Mountains (Cantabrian Region). These mountains, declared National Park since 1995, are basically characterised by a karst relief up to 2600 m altitude and high slopes related to fluvial incision and glacial erosion. Most of the bedrock is Carboniferous limestone and was partially covered by reddish Permian-Triassic sandstone and lutite, preserved nowadays as small outcrops in the lowest areas, for instance in the head of the Sobra valley (Figs. 1C and 2) (Merino-Tomé et al., 2013). These detrital rocks were eroded and transported to inside karst caves formed since, at least, Pliocene times (Fernández-Gibert et al., 2000; Ballesteros et al., 2019). In Sobra Valley, more than 7 km of karst caves dominated by phreatic and vadose passages developed since at least the Middle Pleistocene (Smart, 1984, 1986).

During MIS 3, dry, cold and open landscapes dominated Picos de Europa (Moreno et al., 2010). While humans settled mainly in areas below 300 m altitude around Picos de Europa (e.g. Baena Preysler et al., 2019), glaciers developed in the highest areas, showing a lo-
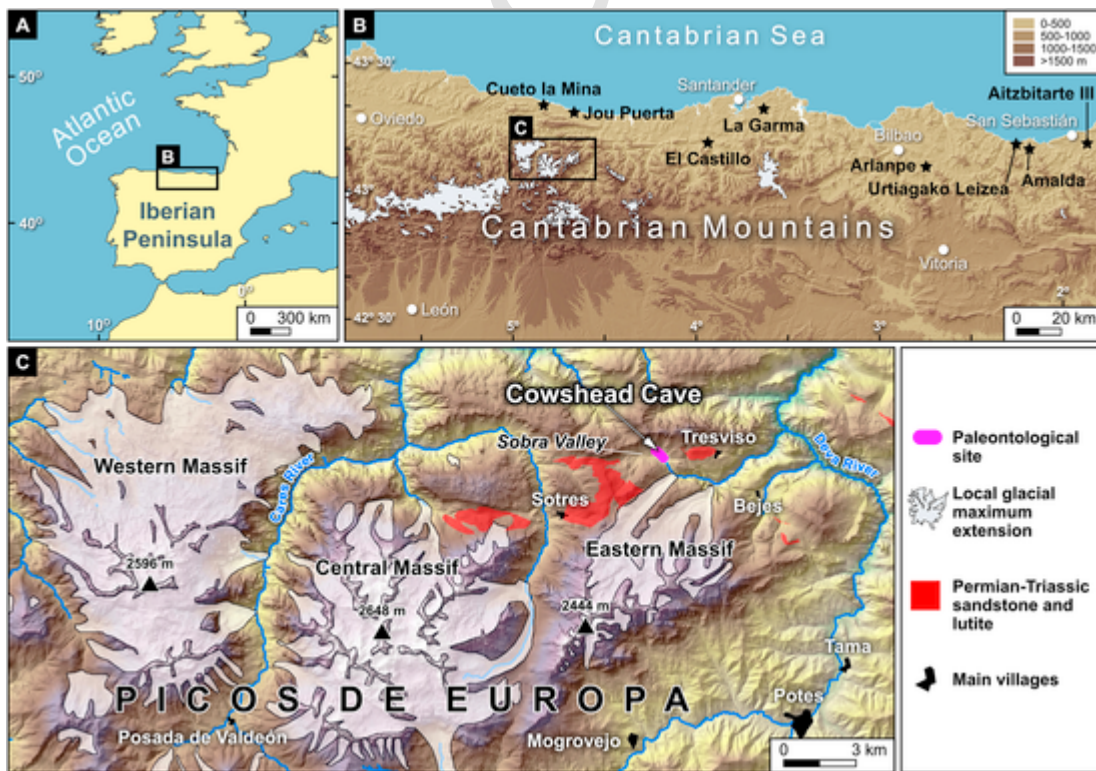

Fig. 1. Location of the Cowshead Cave in the Picos de Europa Mountains, northern Cantabrian Mountains. Local glacial maximum extension is taken from Alonso (1998), Rodríguez-Rodríguez et al. (2014) and Serrano et al. (2017) whilst Permian-Triassic rock outcrops are taken from Merino-Tomé et al. (2013).
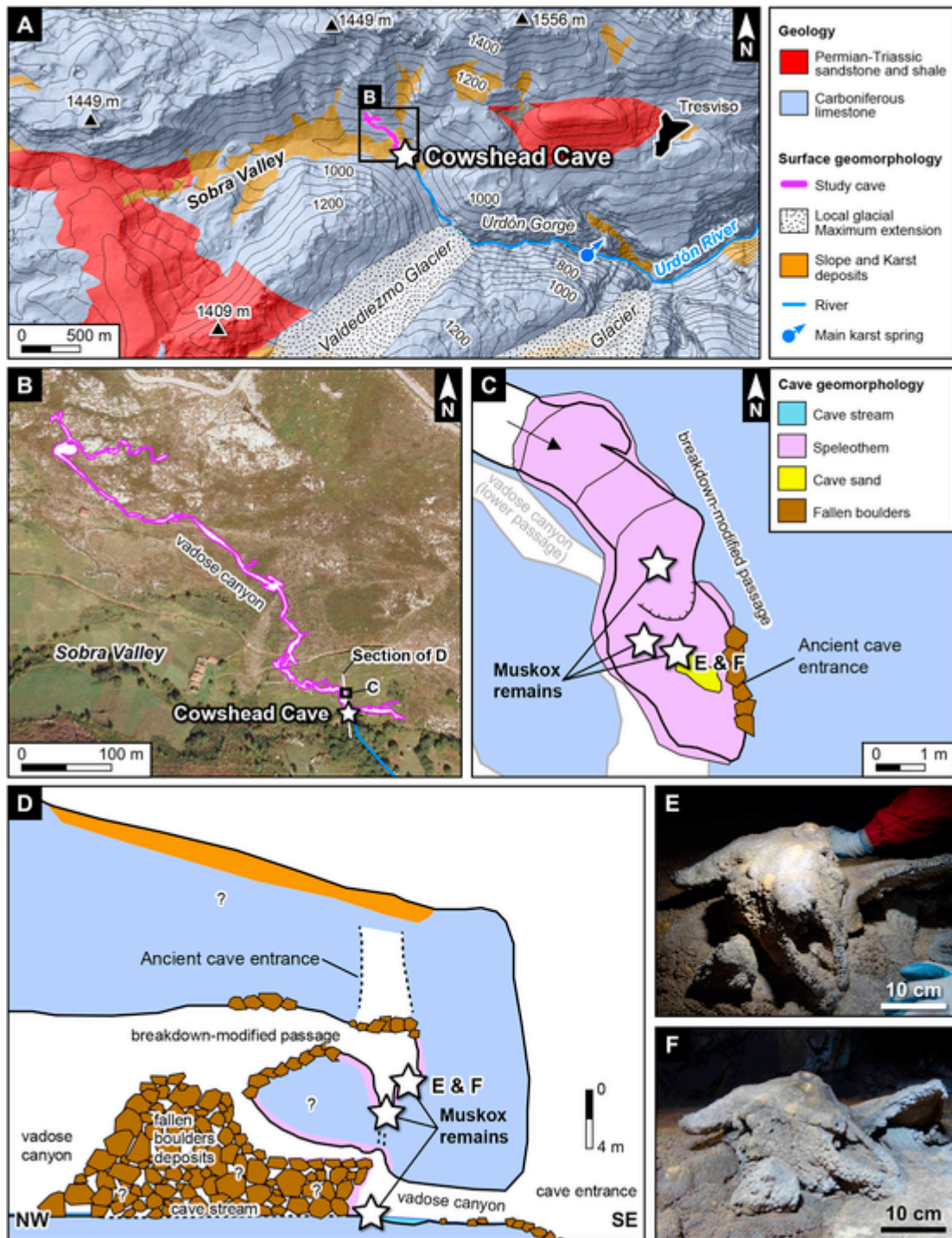
Fig. 2. A, Geology and geomorphology of the surroundings of the Cowshead Cave. B, Projection of Cowhead Cave on the orthophotography. C, Cave geomorphological map of the paleontological site (whose position is shown in B), highlighting the location of the found muskox remains. D, Cross-section (whose position is displayed in B) along the southernmost part of the cave. Anterior view of the muskox skull CH-1 covered by speleothems. F, anterior-lateral view of the skull.

cal maximum extent at around 45 ka (Jiménez-Sánchez et al., 2013). During this maximum, glacier fronts descended to 600–900 m altitude in Picos de Europa (Serrano et al., 2017). In the N of the Eastern Massif, a glacier front would have been located at ~500 m distance from the Cowshead Cave entrance (Fig. 1C). The glaciers did not occupy the entire Sobra Valley, but they blocked its lowest section, at the confluence with the Valdediezmo Valley, during the last local glacial maximum extent (Serrano et al., 2017). Subsequently, during the second half of MIS 3, glacier fronts underwent a general retreat associ-

ated with the development of cold and dry conditions in mountain areas (Moreno et al., 2010; Serrano et al., 2012), with probably minor advances, followed by a noticeable advance associated with MIS 2 (Ruiz-Fernández et al., 2016).

3. Material and methods

3.1. Geomorphology

The geomorphological study of the paleontological site was carried out to establish the origin of the fossil assemblage, using ArcGIS 10.5 to elaborate a geomorphological map of the paleontological site following Ballesteros et al. (2015). Compass software was used to process survey data, allowing us to project the limits of cave deposits and forms onto a topographic survey made using the DistoX laser rangefinder. In order to establish the provenance of the cave sand, its geochemical composition (three samples were taken) was compared with the composition of the Permian-Triassic sandstone of the Sobra Valley bedrock (two samples) and the Carboniferous limestone that hosts the cave under study (two samples). Samples were ground and then pressed mechanically into a metallic cylinder 1.7 cm in diameter and 3 cm long. They were then analysed using a Niton XL3t portable XRF which was previously calibrated using four reference materials. Thirty-three chemical elements were measured and normalized with respect to the composition of the Paleo Archean Australian Shale (PAAS) (McLennan, 2001).

3.2. Mammal paleontology

The large-mammal assemblage comprises 39 fossil remains, all of them corresponding to *O. moschatus*. Fossils are exceptionally well preserved (Figs. 3–5) including an almost complete skull with the left mandible attached (specimen referenced as CH-1, Figs. 3 and 4). A minimum number of two individuals are recognised: 1) the skull and fourteen small-sized and incompletely grown postcranial remains (including vertebrae, scapula, humerus, radius, tibia and astragalus, Fig. 5h–k), correspond to a young individual; 2) other seven larger-sized postcranial remains (comprising scapula, radius, tibia, metacarpal, and phalanges, Fig. 5a–g), presenting a more advanced degree of epiphyseal fusion (although some of them are still not fully grown), correspond to a subadult individual. In addition, seventeen rib fragments, which could not be accurately assigned to any of the two individuals, were recovered.

Most of the fossils were found scattered over the cave floor or partially buried in the few first centimetres of the sediment, so the recovery consisted essentially in a picking-up of the remains, although the skull and a few other elements were covered by flowstone.

For most of the fossils, the preparation consisted basically in the mechanical removal of the adhered sediment. However, others, for instance the skull, required months of exhaustive and careful laboratory work to remove the flowstone cover. All the fossils were subsequently consolidated with Paraloid B-72.

Skull measurements (detailed in Fig. 6) followed the standards described by Von den Driesch (1976) and included some additions of our own. Measurements on teeth and postcranial remains followed Von den Driesch (1976). All measurements were taken with calipers of different sizes and expressed in mm. Teeth nomenclature is detailed in Fig. 7. Aging and sexing of the individuals followed Allen (1913), Tener (1965) and Henrichsen and Grue (1980).

For the comparative study of the CH-1 skull and teeth, the vast collection of recent musk ox remains kept at the Natural History Museum of Denmark (NHMD), which comprises almost 300 skulls originating mostly from Greenland, was studied by DA-L. All the available specimens of similar individual age to CH-1, i.e. those aged between 13 and 26 months (broadly in their second year of life), were selected for this purpose. No data on fossil skulls from young individuals could be included: in the literature on Pleistocene *Ovibos* cranial remains, usually only descriptions and measurements of adult specimens are provided (e.g. Tikhonov, 1998; Raufuss and von Koenigswald, 1999; Stefa-niak et al., 2019); consequently, published information on young individuals is virtually inexistent. For comparison of the postcranial remains, both recent (from Greenland, kept at the Zoological Museum, NHMD) and fossil specimens (from published sources, detailed in Section 5.4) were considered.

In order to recover small-mammal remains, a sample of the sediment containing the musk ox remains was water-screened using superimposed sieves with 2- and 0.5-mm mesh lights. Fossil elements contained in the sediment were recovered by checking with a binocular microscope under 10x magnification. Taxonomic identifications were carried out by means of photographs taken with a parallel-optics type stereo microscope Nikon SMZ800N equipped with a 5 Mpx digital camera. Small-mammal remains resulted very scarce, with only one element suitable for identification (see Section 9).

3.3. Tooth microwear analysis

Tooth microwear patterns were analysed on the two first upper molars (left and right) of the skull CH-1. The sample size is small, but microwear provides dietary information for that specific individual at the time of death. The microwear was quantified using a light stereomicroscope (Zeiss Stemi, 2000C) through direct observation on a 0.16 mm^2 area following the technique established by Solounias and Semprebon (2002). On each molar, the numbers of pits (NP) and scratches (NS) were quantified in two areas and then averaged. Other variables were qualitatively scored: presence/absence of large pits (LP), gouges (G) i.e., circular features with irregular shape, cross scratches (XS) i.e., scratches oriented differently than the majority of scratches, hyper-coarse scratches (HC) i.e., very large scratches, and puncture pits (PP). The width of the scratches was assessed through the Scratch Width Score (SWS) where 0 corresponds to fine scratches, 1 to a mixture of fine and coarse, and 2 to coarse scratches. The microwear pattern was compared with data collected by F.R. on extant specimens from East Greenland (collection housed at the Naturhistorisches Museum Wien), Banks Island (at the Universität Tübingen), Melville Island and Prince of Wales Island (at the Canadian Museum of Nature Ottawa).

3.4. Dating

One bone sample from the right radius of the young individual (CH-5) was selected for AMS radiocarbon dating and sent to the DirectAMS laboratory, North Creek (USA). The age obtained (see Section 9) was calibrated by means of INTCAL 13 database (Reimer et al., 2013) using the software OxCal v.4.3.2 (Bronk Ramsey, 2017), and considering the error as two times the standard deviation (95% probability). This calibrated date is expressed in cal ka BP.

4. Geomorphology and origin of the paleontological site

The entrance of Cowshead Cave is located in the easternmost part of the Sobra karst valley. This valley stands at 800–1250 m altitude, is 3 km long and has an E-W orientation (Fig. 2A). Summits up to 1556 m above sea level surround the valley where karst and slope deposits were identified. This valley is perched above the Urdón Gorge, whose incision has not reached the Sobra Valley at present. The paleontological site is located in the southernmost part of Cowshead Cave, near the cave entrance. This cave is essentially formed by a vadose canyon with a stream flowing along its bottom (Fig. 2B, C and D). This stream emerges at the cave entrance, generating a karst spring. Rockfall processes enlarged the top of the vadose canyon, creating a breakdown-modified passage and the fallen boulder deposits (Fig. 2D). Flowstone, stalactites, draperies and other speleothems covered most of the walls of the breakdown-modified passage, as well as some fallen boulder deposits. The roof of this passage also presents fallen boulders cemented by flowstone (Fig. 2D). The breakdown-modified passage hosts the ac-

Fig. 3. *Ovibos moschatus* skull (CH-1) from Cowshead Cave in dorsal (a), ventral (b), anterior (c), occipital (d), left lateral (e) and right lateral (f) views. Scale bars are in cm.

cumulated faunal assemblage, although a humerus was also found in the cave stream channel. Except for this bone, all fossil remains appeared 7–10 m above the cave stream and 13 m below the topographic surface. The skull, scapula, limb bones and vertebrae were found covered by flowstone (Fig. 2E, F), while astragalus, vertebrae, ribs and other elements were partially covered by uncemented sand sediments (65–80% quartz and 20–35% carbonates according to XRF analyses).

The geochemical compositions of cave sand from the paleontological site, Carboniferous limestone and Permian-Triassic sandstone normalized to the PAAS are shown in Fig. S1 (Appendix A, Supplementary data). In general, the compositional trends of the cave sand and Permian-Triassic sandstone have similarities between them, showing more differences with respect to the Carboniferous limestone. Cave sand and Permian-Triassic sandstone show similar concentrations in As, Au, Cs, Nd, Pb, V, Zn and Zr, which are 1–8 times higher than in Carboniferous limestone. These detrital materials have similar content in La and Nd as well, while these values are higher in the limestone. The cave sand presents a content in Ca closer to the Carboniferous limestone than to the Permian-Triassic sandstone due to the frequent precipitations of carbonates inside the cave. Considering the mentioned evidence, the cave sand probably comes from the erosion of the Permian-Triassic sandstone located at the head of the Sobra Valley (Fig. 2A).

The bone accumulation found in the paleontological site developed due to the fauna falling through an ancient cave entrance that is currently blocked by fallen boulders and speleothems. This ancient entrance was a vertical shaft more than 13 m deep (Fig. 2D), which
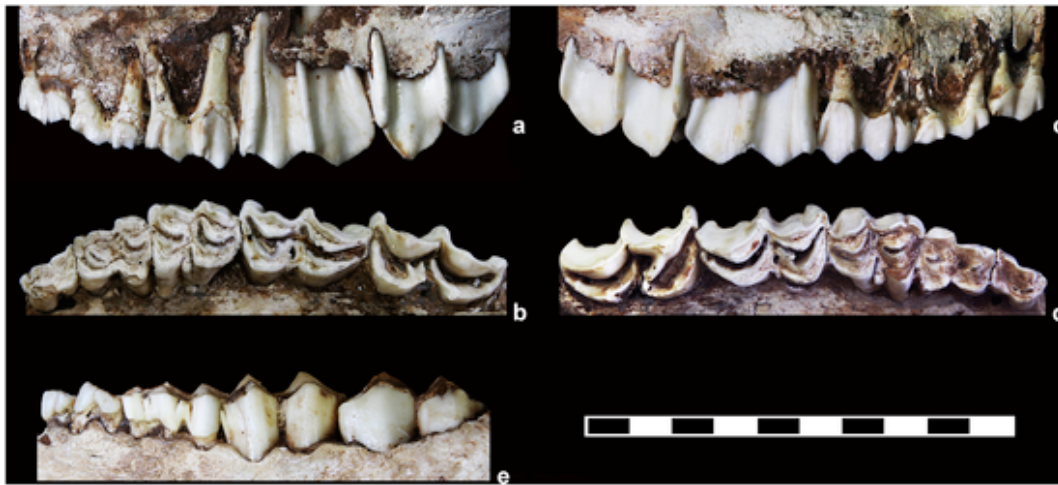
Fig. 4. Dentition of the *Ovibos moschatus* skull (CH-1) from Cowshead Cave: left upper series in labial (a) and occlusal (b) views; right upper series in labial (c) and occlusal (d) views; left lower series in labial view (e). Scale bar is in cm.
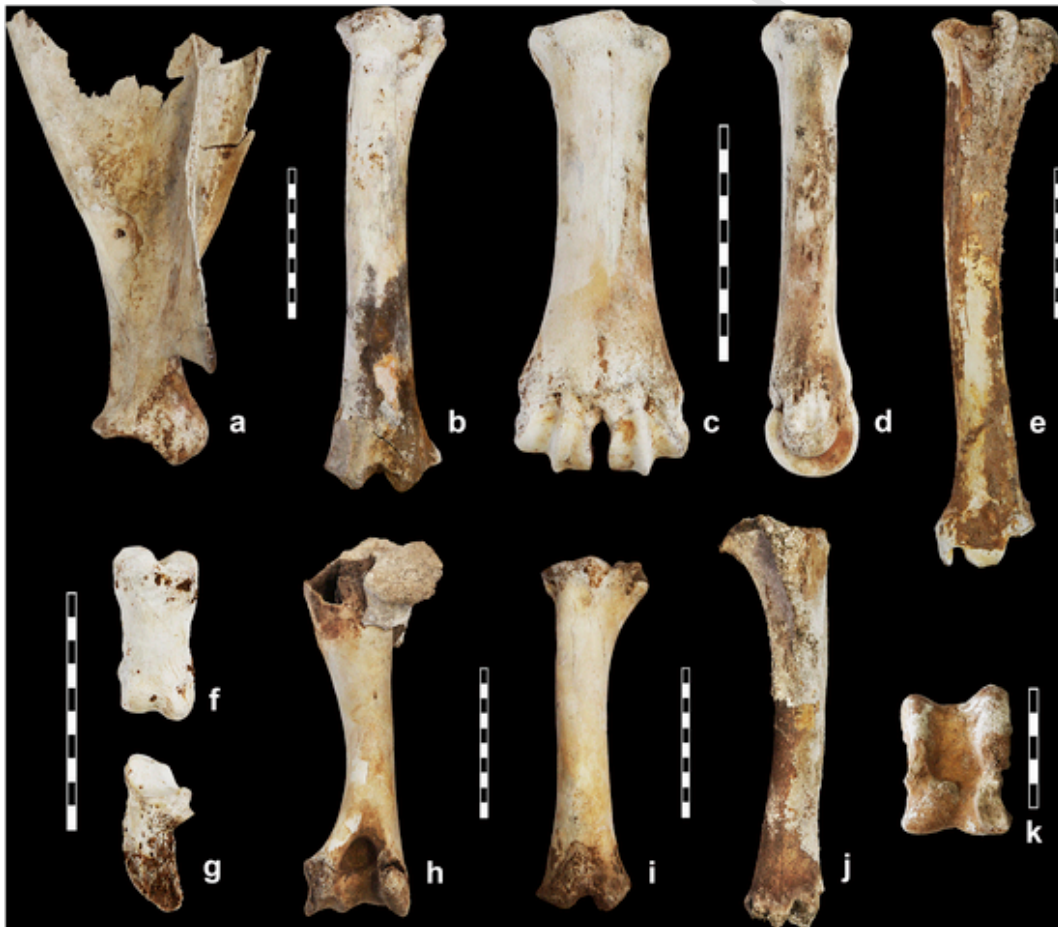

Fig. 5. Postcranial elements of *Ovibos moschatus* from Cowshead Cave. Elements of the subadult individual: right scapula (CH-16) in lateral view (a); left radius (CH-17) in anterior view (b); left metacarpal (CH-20) in anterior view (c) and lateral (d) views; left tibia (CH-19) in anterior view (e); proximal phalanx (CH-21) in anterior view (f); distal phalanx (CH-22) in dorsal view (g). Elements of the young individual: left humerus (CH-3) in posterior view (h); left radius (CH-5) in anterior view (i); right tibia (CH-6) in anterior view (j); left astragalus (CH-7) in anterior view (k). Scale bars are in cm.

acted as a natural trap for musk oxen. The good preservation of the fossils and the lack of any evidence of human or carnivore activity agree with this hypothesis.

Once the fauna fell into the shaft, a humerus and possibly other remains reached the cave stream channel. It is assumed that this stream could destroy some fossil remains. Musk ox accumulation was co-eval with the deposition of quartz sand from the erosion of Permian-Triassic sandstone. Run-off processes transported the sand ~2 km from the head of the Sobra Valley to the ancient entrance of Cowshead Cave (Fig. 2A). Consequently, this valley would present sandy surficial deposits when it was occupied by musk ox populations. Coevally, glaciers would be present only in the highest areas of Picos de Europa (or
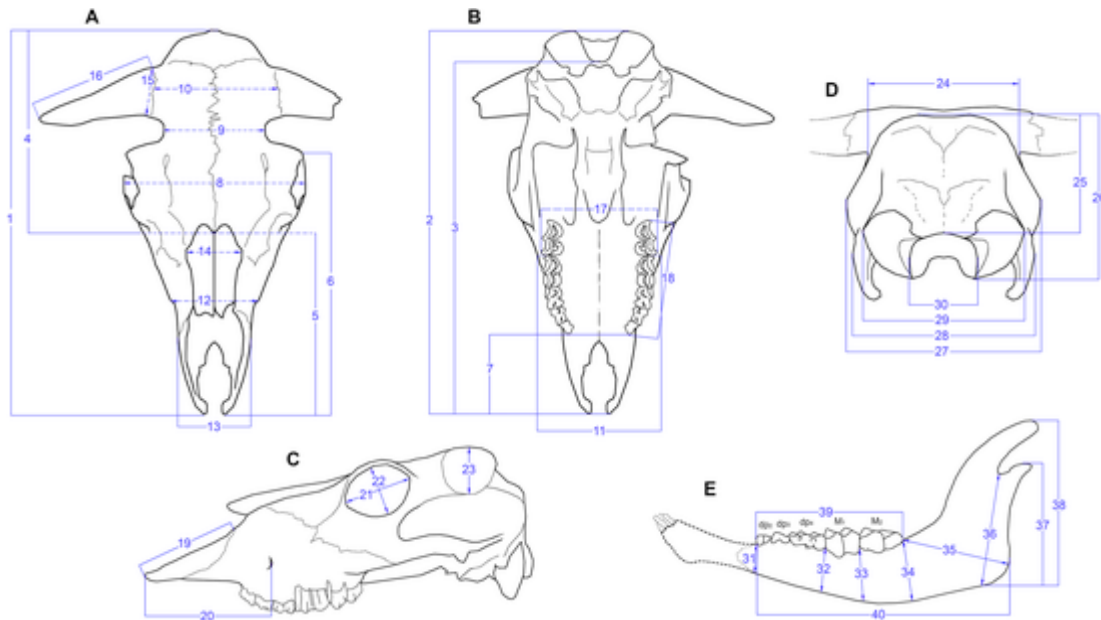
Fig. 6. Scheme indicating the measurements taken in the skull and mandible CH-1. Designation of each measurement is specified in Table 1.

even would not be present), since musk ox habitats are not compatible with the presence of nearby glaciers (Ferguson, 1991). After this, breakdown processes blocked the ancient cave entrance and speleothems precipitated covering the fossil remains.

5. Morphologic and morphometric comparative study of the *O. moschatus* remains

The *O. moschatus* assemblage from Cowshead Cave corresponds to a minimum of two individuals: one young (comprising the skull and a number of small-sized and incompletely grown postcranial remains) and one subadult (including seven larger-sized postcranial remains which show a more advanced degree of epiphyseal fusion, although some of them are still not fully grown). Almost all of these remains were found together in a single assemblage, suggesting that probably they are coeval.

Descriptions and a comparative study of these elements, as well as estimations of their individual age and sex, are provided below. Cranial and postcranial elements from Cowshead Cave were compared to recent musk ox material from Greenland kept at the NHMD (Fig. 8), as well as to fossil specimens from Europe and Siberia (information from published sources).

5.1. Skull description

The skull CH-1, which corresponds to the young individual, is exceptionally well preserved except for the left horn core, which is partially missing, and the damaged right zygomatic arch. In addition, some parts show superficial erosion. The individual age of the specimen was estimated to be about 20 months (see Section 6).

The skull's general shape in dorsal view is slender, with protruding eye orbits, narrow frontal bone and a pronounced postorbital constriction (Fig. 3a), which is distinctive of *Ovibos*.

The orbits show a wide and deep depression in the anterior border, the so-called "lacrymal pit" or "lacrymal groove", which is well visible in the left orbit (Fig. 3a) while the right one is slightly damaged. This trait was also observed at all the studied recent skulls from Greenland and is described by some authors such as Lönnberg (1900), Allen (1913) and Crégut-Bonnoure (2002) as a typical feature of *Ovibos*.

Anteriorly to the orbits, the skull is broad compared to the recent specimens from Greenland (Fig. 8a–c). This is because CH-1 shows al-

most no constriction in front of the orbits (anteorbital constriction), giving it a particular triangular (or horse-like) shape in the rostral area, while in the recent specimens this constriction is quite marked (Fig. 8b and c). In order to quantify this morphological peculiarity, CH-1 was compared to other young skulls of similar individual age: 13 of the modern *Ovibos* skulls from Greenland kept at the NHMD correspond to individuals aged between 13 and 26 months old, so they were considered suitable for this comparison. Two measurements of width from the rostral area (the greatest width of the premaxillaries, in the anterior edge, and the width at the level of the M^1-M^2 boundary, in the posterior margin, see numbers 13 and 11, respectively, in Fig. 6) were taken and plotted in Fig. 9A. CH-1 is located at the right border of the graph, clearly separated from the recent sample, denoting a much greater width in the posterior edge of the rostral area (right in front of the orbits) relative to the anterior portion. Even in the recent sample, males and females are plotted separately due to the greater width of male skulls.

The nasal bones are damaged, showing some superficial erosion and lacking the nasal processes. The premaxillaries are slim, becoming narrower anteriorly and ending in a pointed shape. Their posterior edge does not contact the nasals.

The postorbital constriction (corresponding to the minimum frontal width) is noticeably more pronounced in CH-1 than in modern young specimens from Greenland (Fig. 8a–c), which is another peculiarity of this skull. The average value of the ratio Greatest length/Minimum frontal width, calculated in the modern population (n = 13) is 3.4 (males = 3.27; females = 3.55), while for CH-1 this ratio is 3.93, indicating a more pronounced narrowing in this area. These variables are plotted in Fig. 9B, where it can be seen that males and females of the modern population follow different trends (males show a much greater dispersion). The skull CH-1 is located in the highest part of the diagram, far from the trends of the modern specimens.

The horn cores show a slight dorsoventral flattening. While the right one is well preserved, the left one is incomplete. In dorsal view (Fig. 3a), the right horn core is straight and arranged almost perpendicular to the longitudinal axis of the skull, slightly onward. In occipital view (Fig. 3d), it is deflected about 13° down from the horizontal, with the apical portion curving slightly upward. The parietal and the nuchal crest extend backward and downward from the horn bases (Fig. 3a, e, f). The postero-frontal and parietal regions are not covered
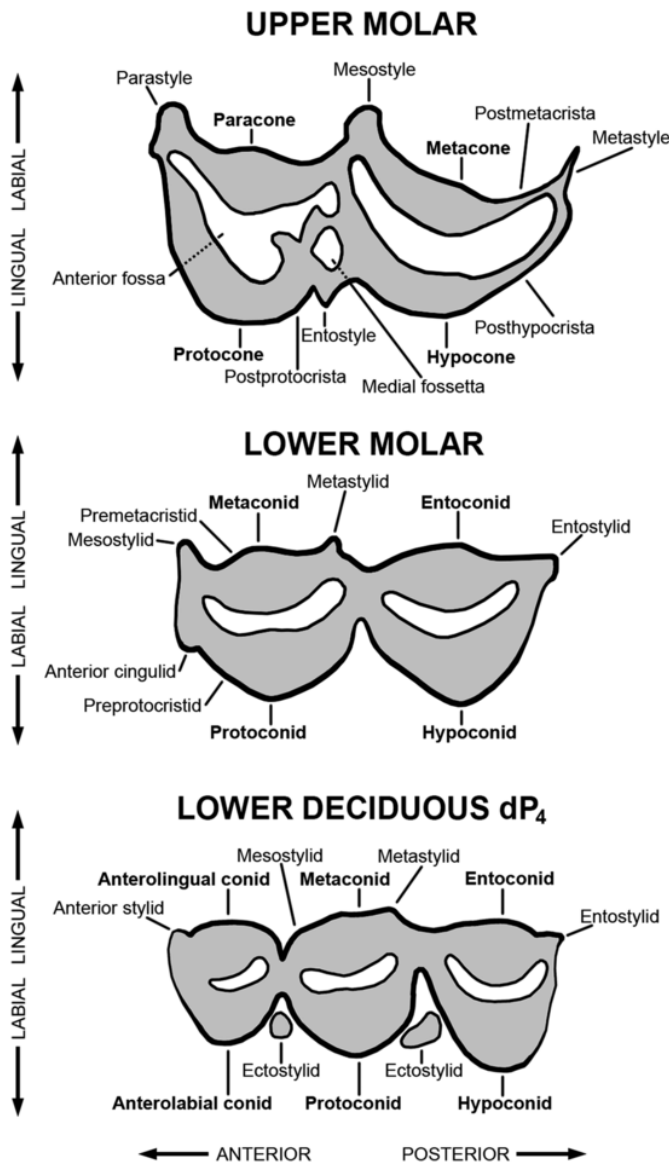
UPPER MOLAR

LOWER MOLAR

LOWER DECIDUOUS dP₄

Fig. 7. Teeth nomenclature: principal structures and other dental elements cited in the text of upper molars, lower molars and lower deciduous dP_4.

by the characteristic rough exostosis of the *Ovibos* adult skulls, indicating that this individual was a young one.

The infraorbital foramen is double in the right side and single in the left side (Fig. 3c). In the studied sample of recent musk ox from Greenland, the number of infraorbital foramina is variable: single or double is the most frequent pattern, while occasionally they showed three foramina and, exceptionally, four. These foramina open rather back compared to other bovids, as previously noted by Lönnberg (1900): in CH-1, they are located above the dP^3-dP^4 border (Fig. 3e and f), exactly the same position as in the other 13 studied recent skulls of young specimens from Greenland. This feature is preceded by other small additional foramen located over the dP^2, which was also observed at all the studied *Ovibos* skulls from Greenland, always located over the first tooth of the row (dP^2 in young specimens and P^2 in adults). The presence of this additional foramen in *Ovibos* was described by Crégut-Bonnoure (2002).

The palatal surface is concave. The suture between palatines and maxillae is wavy, since each palatine has two lobes (in median and lateral positions) extending forward at both sides of the palatine foramen, as described by Lönnberg (1900).

The general size of the CH-1 skull (see measurements in Table 1) was compared to the mentioned sample of 13 skulls of modern young individuals from Greenland. The greatest length of the skull is plotted against the greatest width (Fig. 9C) and the condylobasal length against the width at the mastoid area (Fig. 9D): among the recent sample, males are noticeably larger than females; however, there is not a clear correlation between size and age, since the larger specimens are not the older ones (the largest male is aged 16–18 months), denoting individual variability. The CH-1 specimen is the largest one of the whole sample, which is of special interest considering that it was compared with some specimens of even older individual age (the estimation of the individual age of CH-1 is discussed in Section 6.1). Only one of the recent specimens showed a slightly greater width at the mastoid area (Fig. 9D).

5.2. Mandible

Only the left hemimandible of the CH-1 skull was recovered (Fig. 3e). The anterior portion, including the symphysis, the anterior teeth and almost all the diastema, is lacking. The lower cheek teeth, comprising dP_2, dP_3, dP_4, M_1 and M_2, are preserved. In the posterior portion, it can be observed that the coronoid process is strongly curved backwards, which is a characteristic trait of *O. moschatus*, as noted by Lönnberg (1900) and Crégut-Bonnoure (2002).

5.3. Teeth

The morphology of the dentition of skull CH-1 (Fig. 4) is typical of *Ovibos*, resembling that of caprines like *Capra* or *Ovis*, but with some features more comparable with those of bovines.

All the teeth lack any trace of cement, which is also typical of caprines such as *Ovis* and different from bovines like *Bison* (whose molars are usually covered by cement). In occlusal view, the upper molars are longer than broad and show a median fossetta, which are characteristic features of *Ovibos*. In the labial side, the styles (parastyle, mesostyle and metastyle) are prominent, while the surfaces between them are almost flat. These features also resemble those of caprines and are different from those of bovines, which show less prominent styles and convex surfaces between them (Khan, 1966; Mol and Zijlstra, 1994). In the lingual side, the upper molars show small entostyles or median pillars, which are also present in bovines (though more developed) and absent in caprines as *Ovis* and *Capra* (according to Allen, 1913). This feature is also present in some of the deciduous teeth, as we will describe below. Lower molars M_1 and M_2 lack median pillars (ectostylids), as is distinctive of *Ovibos*.

A more detailed description of each tooth is provided below. Dental nomenclature is specified in Fig. 7.

dP^2. The occlusal surface is extremely worn out, almost no enamel remains. Their general morphology is rectangular, as was typical for the recent individuals from Greenland.

dP^3. The crown is very worn. Both lobes are clearly asymmetric: the anterior one is square, while the posterior one is much shorter and broader. This morphology is identical to that of the dP^3 of the studied recent specimens from Greenland.

dP^4. The wearing degree is slightly lower than in the other deciduous teeth. The occlusal surface shows a small median fossetta, which is barely visible in the right specimen. A particularity observed in both dP^4 is the presence of well-developed entostyles or median pillars located between protocone and hypocone (Fig. 4b, d). This structure is teardrop-shaped in occlusal view, elongated labio-lingually and connected to the protocone, resembling the shape of the pillars described by Khan (1966) for the upper molars of the specimen ascribed by him to *Ovibos pallantis rhenanus*. This trait is remarkable in the Cow-
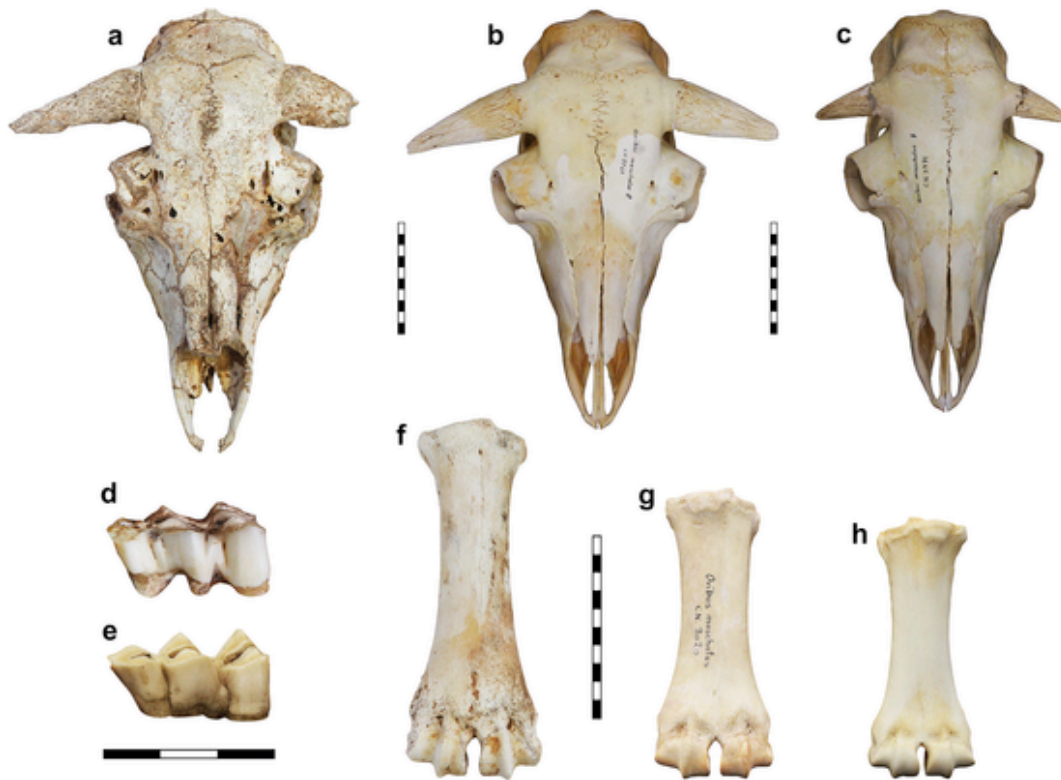
Fig. 8. Comparison of *Ovibos moschatus* skull, dP$_4$ and metacarpal from Cowshead, with modern specimens from Greenland kept at the Zoological Museum, Natural History Museum of Denmark: skull of Cowshead Cave (CH-1) in dorsal view (a); modern skull of a 20 months-old male from Greenland (CN. 3763) in dorsal view (b); modern skull of a 20 months-old female from Greenland (CN. 3774) in dorsal view (c); left dP$_4$ from Cowshead Cave (of skull CH-1) in labial view (d); modern left dP$_4$ from Greenland (CN. 3474) in labial view (e); left metacarpal of Cowshead Cave (CH-20) in anterior view (f); modern left metacarpal of an adult male from Greenland (CN. 3020) in anterior view (g); modern right metacarpal of an adult female from Greenland (CN. 3778) in anterior view (h). Scale bars are in cm.

shead specimen since entostyles are poorly developed or absent in the dP4 of the studied recent specimens from Greenland.

M^1. This molar is fully grown and in wear: dentine is exposed at all the cristas except in the posterior ones (posthypocrista and postmetacrista), where wearing is very slight.

In occlusal view, the molar length almost doubles its width (see measurements in Table 2). Median fossettas are well developed in both the left and right specimens. Parastyle, mesostyle and metastyle are very prominent, while the interstylar faces are nearly flat. No trace of cingulum is observed. Entostyles are present as in *Bison* and *Bos*, though rather less developed (Fig. 4b, d), as is typical for *Ovibos*, according to Allen (1913). Entostyles are not in central position, but slightly displaced anteriorly toward the protocone. In occlusal view, they are triangular-shaped. In all the described morphological features, M^1 from CH-1 skull are indistinguishable from those from the studied recent musk ox from Greenland.

M^2. The crown is totally unworn. The thin bone wall of the lateral side of both maxillaries is clearly damaged, giving the erroneous impression (in lateral view) that M^2 were completely erupted. In order to assess the real erupting degree of the M^2, we must focus on the rise of its crown with respect to M^1 (Fig. 4a, c). In the anterior half, the paracone rises at the same level of the M^1, while the protocone is slightly below. The posterior half (metacone + hypocone) is visibly below, with the hypocone just starting to emerge above the alveolar border. The morphology of the crown is very similar to the M^1: antero-posteriorly elongated, with very prominent labial styles and nearly flat interstylar faces. Since the occlusal surface is unworn, median fossettas are not well defined. Due to the incipient stage of emersion of the lingual side, entostyles are not yet visible. The right M^2 shows a pathology: an extra enamel fold diagonally crosses the anterior fossa, from the middle of the paracone's lingual face towards the posterior end of the postpro-

tocrista (Fig. 4d). This peculiar feature is not present in the left M^2 of the same skull nor in any of the studied recent specimens from Greenland.

dP$_2$. The wearing stage is very advanced. The morphology of the occlusal, lingual and labial faces is identical to that of the recent dP$_2$ sample from Greenland.

dP$_3$. This tooth also shows advanced wearing. The crown is damaged in the lingual side, so the morphology of the occlusal surface cannot be properly observed. However, the preserved portion is indistinguishable from those of the studied recent dP$_3$ sample from Greenland.

dP$_4$. The wearing degree is slightly lower than in the dP$_3$. An interesting peculiarity is observed: two pillars or ectostylids, well developed and clearly independent of the labial conids, are present in the labial side (Figs. 4e and 8d). This trait is of special relevance, since it does not occur at any of the revised recent dP$_4$ from Greenland. The pattern in the studied recent specimens ranges from total absence of pillars to, at most, slight bulges (Fig. 8e), but well-developed ectostylids such as those of the specimen from Cowshead Cave were not noticed in any case. Specimens from Northern Canada figured by Allen (1913), also lack pillars. Therefore, this is, to our knowledge, the first reported presence of well-developed ectostylids in dP$_4$ from any fossil or modern *Ovibos moschatus* population.

M$_1$. This molar is fully erupted and in wear. The wearing degree is slightly more advanced than in upper M^1, exposing the dentine at all the cristids. In general, the erupting and wear degrees are more advanced in the lower than in the upper teeth of each individual, which is observable both in the Cowshead specimen and in the modern ones from Greenland. The lingual face is relatively flat (stylids are not very prominent) except for a constriction between metaconid and entoconid, which is noticeable in occlusal view. In the labial side, an anterior cingulid is well developed. The ectostylid is absent, which is a typical
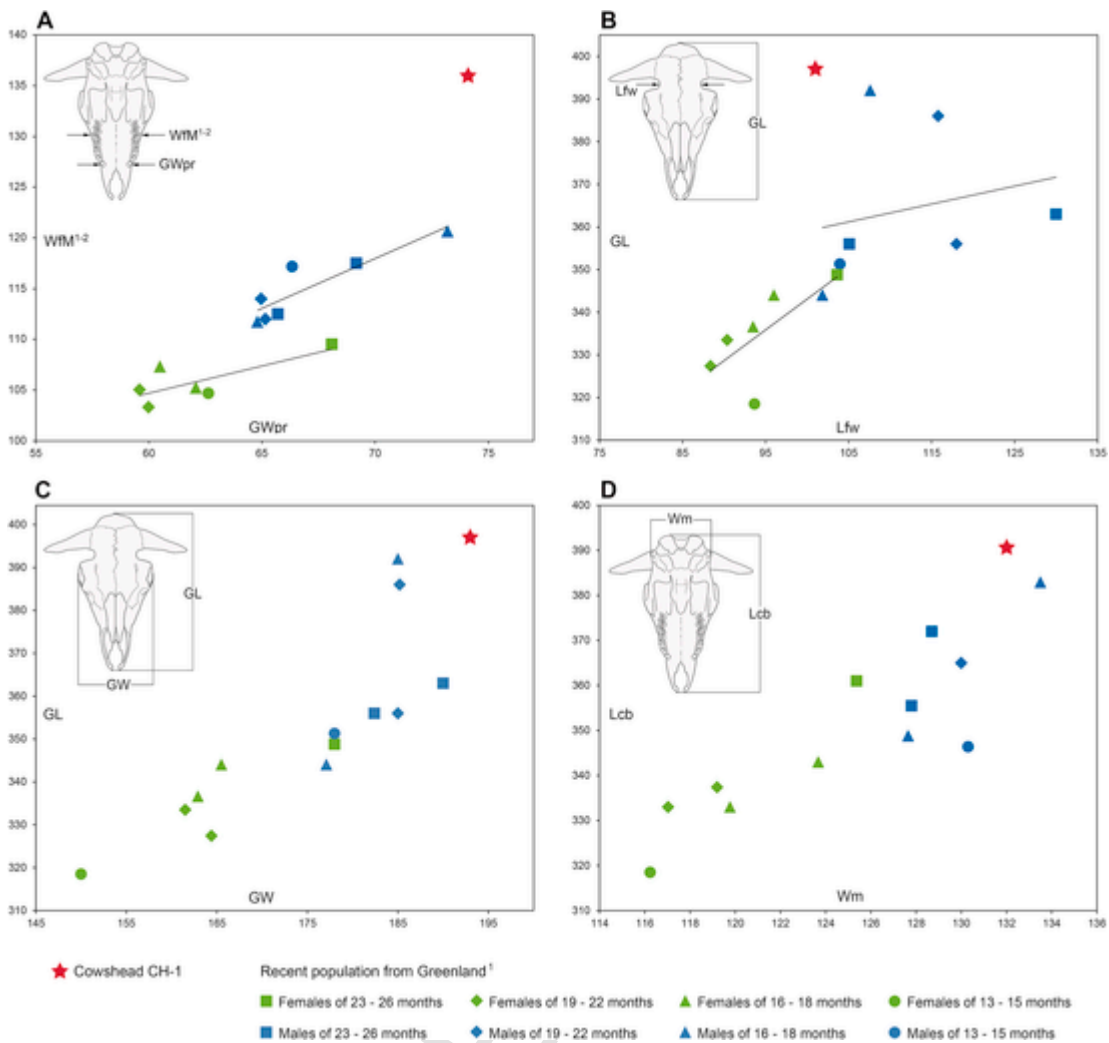
Fig. 9. Bivariate plots of different measurements of *O. moschatus* skull from Cowshead Cave (CH-1) in comparison with modern skulls of young individuals (aged between 13 and 26 months) from Greenland, kept at the Natural History Museum of Denmark: A, facial width at the level of M^1-M^2 boundary (WfM$^{1-2}$)/greatest width of the premaxillaries (GWpr); B, least frontal width (Lfw)/greatest length (GL); C, greatest length (GL)/greatest width (GW); D, condylobasal length (Lcb)/mastoid width (Wm). Source: 1, own data D.A.-L. All measurements are in mm.

trait of *Ovibos* lower molars. Their general shape is identical to that of the modern M_1 from Greenland.

M_2. The erupting degree is more advanced than in the upper M^2: the metaconid is totally erupted and rises at the same level of M_1, while the protoconid is slightly below. The distal cusps (entoconid and hypoconid) are almost totally emerged but still below the proximal ones. A slight wear is present only in the premetacristid and preprotocristid. The morphology is very similar to that of the M_1, with absence of ectostylid and presence of anterior cingulid (while less marked). In general, this molar is indistinguishable from the modern M_2 sample from Greenland.

Teeth measurements are provided in Table 2. For morphometric comparisons, deciduous teeth were not considered useful because their crowns show noticeable shortening due to the advanced interdental attrition. Taking reliable measurements in M^2 was not possible because they were not totally emerged. Consequently, M^1 were selected for comparative purposes since they are the only dental elements that were fully emerged and not yet affected by interdental attrition at the time of death. They were compared to a sample of 26 recent M^1 from Greenland: only M^1 of individuals in roughly their second year of life (from 13 to 26 months of age) were considered because they are fully grown but still not affected by interdental attrition at this stage. The results are shown in Fig. 10 and indicate that both left and right M^1 of

the CH-1 skull are the widest ones of the whole sample. Moreover, the left M^1 is also the longest one, while the right one (which is slightly shorter) is only surpassed in length by one specimen of the recent sample from Greenland.

5.4. Postcranial remains

A total number of 38 postcranial elements were recovered in the assemblage. Those corresponding to the young individual (Fig. 5h–k) include eight vertebrae, one scapula fragment, two humeri, one radius, one tibia and one astragalus. The subadult assemblage (Fig. 5a–g) comprises one scapula, one radius, one tibia, one metacarpal, one proximal phalanx and one distal phalanx. In addition, 17 rib fragments, which could not be accurately assigned to any of the two individuals, were recovered. With the exception of the metacarpal, which is described in detail below, the musk ox postcranial remains from Cowshead Cave do not show any morphological particularity when compared to the sample of recent specimens from Greenland.

Most of the bones show incompletely fused epiphyses and diaphysis (see detailed information in Sections 6.1.4. and 6.2.1.), indicating that they were still growing when the animals died. Consequently, only the metacarpal (CH-20; Fig. 5c and d), scapula (CH-16; Fig. 5a) and pha-

Table 1
Measurements (in mm) of the skull and mandible CH-1. The numbers correspond to the measurements specified in Fig. 6.

Number	Measurement	CH-1
1	Greatest length of the skull (Prosthion - Akrokranion).	397
2	Condylobasal length.	390.7
3	Basal length.	363.5
4	Medial frontal length (Akrokranion - Nasion).	213.5
5	Length Prosthion - Nasion.	183.5
6	Length Prosthion - posterior edge of the orbit.	268
7	Length Prosthion - anterior border of dP^2.	97.5
8	Greatest width of skull.	193
9	Least frontal width (=postorbital constriction).	101
10	Width between the bases of the horn cores.	105
11	Facial width at the level of M^1-M^2 boundary.	136
12	Facial width across the tuberosities.	128
13	Greatest width of the premaxillaries.	74.1
14	Greatest width across the nasals.	51
15	Anteroposterior diameter at horn core base.	48.9
16	Greatest length of horn core.	120
17	Greatest palatal width between the lingual borders of M^2.	113.6
18	Length of the cheekteeth row (dP^2-M^2).	115.3
19	Lateral length of the premaxilla (Prosthion - Nasointermaxillare).	111
20	Length Prosthion - infraorbitale foramen.	128
21	Greatest inner length of the orbit.	61.8
22	Greatest inner height of the orbit.	53.7
23	Dorsobasal diameter at horn core base.	44.4
24	Least occipital width.	86.6
25	Least height of the occipital region (Opisthion-highest point of nuchal crest).	74.3
26	Greatest height of the occipital region (from the condyles basis to the nuchal crest).	103.7
27	Greatest mastoid width.	132
28	Greatest width at the bases of the paraoccipital processes.	115
29	Greatest width of the occipital condyles.	102
30	Greatest width of the foramen magnum.	35.9
31	Height of the mandible in front of dP$_2$.	32.1
32	Height of the mandible behind dP$_4$.	42.7
33	Height of the mandible behind M$_1$.	50.5
34	Height of the mandible behind M$_2$.	63
35	Length Gonion caudale - aboral border of alveolus of M$_2$.	95
36	Height from Gonion ventrale - deepest point of the mandibular notch.	111
37	Height from Gonion ventrale - highest point of the condyle process.	116.5
38	Height from Gonion ventrale - Cronion.	160
39	Length of the cheekteeth row (dP$_2$-M$_2$).	110
40	Length oral border of dP$_2$ - Gonion caudale.	204

langes (CH-21, CH-22; Fig. 5f and g) of the subadult individual were useful for morphometric purposes (see measurements in Table 3), because they are the only recovered elements with completely fused epiphyses, so we assume that they were totally grown at the time of death.

The morphology of metacarpal CH-20 is distinctive: the diaphysis is narrower in its proximal half while the distal half shows a progressive widening that reaches its maximum at the distal edge (Fig. 5c). This shape is identical to that of the Pleistocene *Ovibos* metacarpals figured by Kahlke and Kahlke (1969), Siegfried (1982), Bosscha Erdbrink (1983) and de Vries (1990). In this aspect, *Ovibos* metacarpals are visibly different from those of other similar species such as bison, whose shaft maintains a constant width for most of its length and widens abruptly near the epiphyses.

The size of metacarpal CH-20 was compared to a sample of Pleistocene specimens from Europe and Siberia and to a sample of recent specimens from Greenland (Fig. 11A). A remarkable difference is noted: Pleistocene specimens (including CH-20) are noticeably larger than recent ones, with no overlap between both populations (Fig. 8f–h). Specimen CH-20 is one of the largest in the entire sample. In addition, the Pleistocene specimens are proportionally longer than the recent ones (Fig. 8f–h): the average value of the ratio greatest length/proximal width in the Pleistocene population (n = 12) reaches 3.2 (the value for CH-20 is 3.28), while in the recent sample from Greenland (n = 66) it is 2.89. Authors like Soergel (1941), Kahlke and Kahlke (1969), Tikhonov (1998) and Crégut-Bonnoure (2002), previously realised that Pleistocene *Ovibos* metacarpals are relatively long and narrow compared with recent ones. Ungulate metapodials show a significant intraspecific variability, which was noticed in many species, mostly in cervids, and is related to adaptation to the landscape along a wide spectrum of habitats and to different lifestyle options (Klein, 1964; McMahon, 1975; Nieminen and Helle, 1980; Klein et al., 1987; Kuzyk et al., 1999; Putman and Flueck, 2011). Such a high plasticity of phenotypic expression in response to different ecological and social circumstances may involve epigenetic factors (Flueck and Smith-Flueck, 2011; Putman and Flueck, 2011).

Morphologically, all other postcranial elements are indistinguishable from the studied *Ovibos* recent sample. It is interesting to remark the low and wide morphology of the distal phalanx, which is very different from those of other bovines and caprines and resembles that of *Rangifer*, as previously noted by Crégut-Bonnoure (2002).

From a morphometric perspective, the scapula and phalanges of the subadult specimen from Cowshead Cave are noticeably larger than those of the recent population from Greenland (Fig. 11B, C, D). This is especially marked in the phalanges: the proximal one is much larger than the entire recent sample (n = 39; Fig. 11C); the distal phalanx is also longer than the whole modern sample (n = 36) and only one of the recent specimens is slightly wider.

6. Aging and sexing of the *O. moschatus* individuals

The age and sex of both the young and the subadult individuals were estimated based on different traits such as teeth erupting and wearing degree, horn core developing, cranial morphology and size, and bone fusion degree. Results and discussion are provided below.
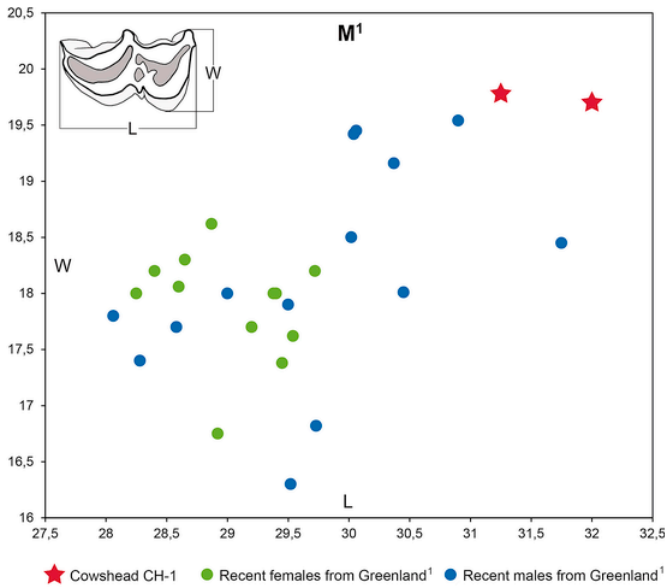
Table 2
Measurements of the upper and lower dentition of skull and mandible CH-1. Width measurements at M^2 and M$_2$ were not able to be taken since these teeth are not totally emerged.

Upper dentition	dP^2		dP^3		dP^4		M^1		M^2
	Length	Width	Length	Width	Length	Width	Length	Width	Length
Left series	15.25	10	19.1	16.45	22.75	20.65	32	19.7	34.16
Right series	14.9	9.9	19.3	15.5	23.2	20.8	31.25	19.78	34.3
Lower dentition	**dP$_2$**		**dP$_3$**		**dP$_4$**		**M$_1$**		**M$_2$**
	Length	Width	Length	Width	Length	Width	Length	Width	Length
Left series	10.3	6.2	13.1	8	28.15	12.8	29.7	12.5	34.8

Fig. 10. Bivariate plot width (W)/length (L) of *O. moschatus* M[1] from Cowshead Cave (of skull CH-1) in comparison with modern specimens from Greenland kept at the Natural History Museum of Denmark. Source: 1, own data D.A.-L. All measurements are in mm.

6.1. Young individual

The young specimen includes the complete skull and a number of postcranial elements indicated in Section 5.4. In order to assess the individual age of the CH-1 skull, two main variables were considered: teeth eruption and wearing, and horn core development. Other variables like skull size and bone suture fusion were also taken into account.

6.1.1. Tooth eruption and wear

While detailed information on each individual tooth is indicated in Section 5.3, a general vision is here provided. All deciduous teeth are still present and heavily worn: the occlusal surfaces of dP^2 show very small remnants of enamel, while in dP_2 any trace of enamel was totally worn out, so only dentine is preserved; in dP^3 occlusal surfaces, small enamel patches are still present, while the dP_3 crown is damaged lingually, so no proper observations could be made; the wearing stage of dP^4 and dP_4 is less advanced, preserving visible enamel isles. Both M^1 are totally erupted, with all the occlusal enamel surfaces in wear. While wearing is advanced in paracone and protocone, as well as in the anterior surfaces of metacone and hypocone, the posterior surfaces of these last cusps (posthypocrista and postmetacrista) are slightly worn (the dentine here is not exposed, Fig. 4b, d). M_1 is also totally erupted, with all the occlusal enamel surfaces showing more advanced wearing than M^1. Both M^2 remain completely unworn. Apparently, M^2 seem to be completely erupted (Fig. 4a–d), but this is only an erroneous impression due to the damage of the external thin bone walls of both maxil-

laries, as discussed in Section 5.3. The erupting degree of M_2 is more advanced than M^2, with slight, barely noticeable wear only in the premetacristid and preprotocristid.

This degree of teeth eruption and wear matches exactly that of the studied modern specimens from Greenland aged 20 months at death. Compared to the descriptions and pictures provided by Allen (1913), Tener (1965) and Henrichsen and Grue (1980), the erupting and wearing degree of CH-1 is slightly greater than that of the individuals aged 18 months.

6.1.2. Horn core development

The right horn core of skull CH-1 in dorsal view (Fig. 3a) is straight and arranged almost perpendicular to the longitudinal axis of the skull, slightly onward, as indicated in Section 5.1. Its length is approximately 1/3 of the skull's greatest length. In occipital view (Fig. 3d), it is arranged sub-horizontally. This morphology is the same as that of the 20 months-old male skulls of the studied modern population from Greenland. It is also very similar to that of the 18 months-old male skull pictured by Henrichsen and Grue (1980), and that of the 18 months-old male skull photography published by Allen (1913).

From a morphometric perspective, the CH-1 horn core was compared with a population of 20 months-old modern individuals from Greenland (n = 4; own data) and with a population of 18 months-old modern individuals from Canada (n = 5; Allen, 1913): the anteroposterior diameter at the base in males is 41–46 mm while in females is 24–34 mm; total length in males ranges from 103 to 115 mm and in females from 45 to 63 mm. CH-1 measurements (anteroposterior diameter at base = 48.9 mm, length = 120 mm) slightly exceed the values of the males from the comparison samples.

In order to evaluate the size of the horn core with respect to the skull, the ratio Greatest length of the skull/Length of the horn core was considered. The values for modern young individuals (18–20 months old) of the above indicated populations from Canada and Greenland range between 3.3 and 3.67 for males and from 5.3 to 6.9 for females. The result obtained for CH-1 is 3.3, matching the male ratio.

The CH-1 horn core is deflected about 13° down from the horizontal, with the apical portion curving slightly upward (Fig. 3d). Such low deflection angle is equal to those measured in the 20 months-old male modern skulls from Greenland. Allen (1913) indicates that the deflection of the horn axis from the horizontal in 18 months-old individuals from Canada is of about 7°. However, the angle measured over the photograph of an 18 months-old male skull published by this author is higher, of about 13–14°, matching the value of skull CH-1. These sub-horizontal angles are typical of specimens under 24 months of age. At two years, the deflection is noticeably more pronounced, reaching values of about 20° in males and 33° in females (Allen, 1913). As individuals get older, this angle increases.

6.1.3. Other skull features

The CH-1 skull, as indicated in Section 5.1 and Fig. 9c and d, is bigger (in most of the measurements) than the 13 skulls of modern young individuals from Greenland, although it is closer to the size of the males, which supports its attribution to a male. Its length (397

Table 3
Measurements (in mm) of postcraneal elements from Cowshead Cave: only fully-grown elements of the subadult individual are considered. Abbreviations: GLP - greatest length of the Processus articularis; WG - width of the glenoid cavity: SLC - Smallest length of the Collum scapulae; GL - greatest length; Wp - width of the proximal end; Dp - depth of the proximal end; Wd - width of the distal end; Dd - depth of the distal end; SD - smallest width of the diaphysis; GW - greatest width.

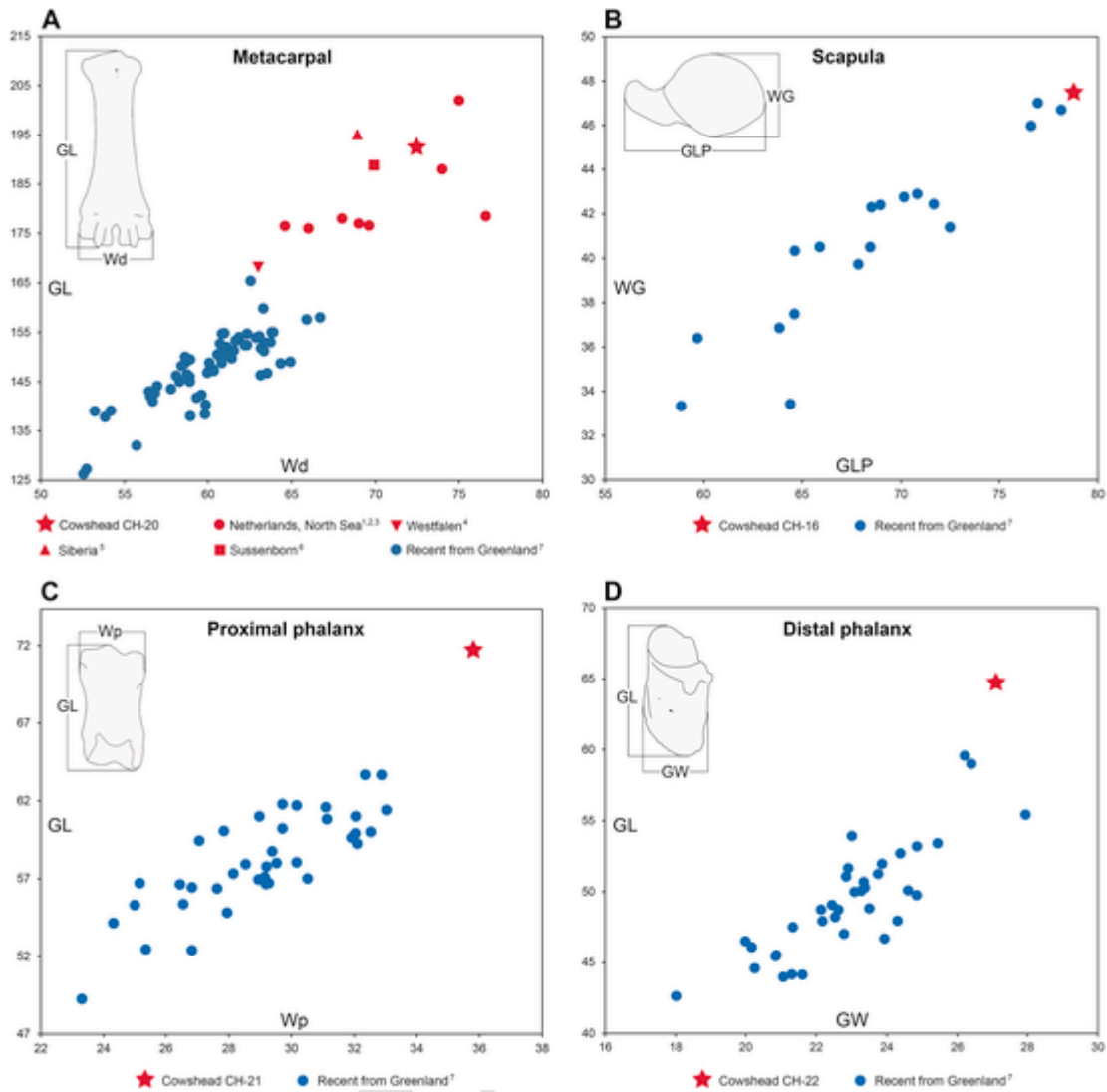| Element	Ref.	GLP	WG	SLC	GL	Wp	Dp	Wd	Dd	SD	GW
Scapula	CH-16	78.76	47.46	47.33							
Metacarpal	CH-20				192.6	58.7	36.4	72.45	35.97	37.4	
Proximal phalanx	CH-21				71.72	35.81	32.85	33.02	22.4	28.3	
Distal phalanx	CH-22				64.73						27.1

Fig. 11. Bivariate plots showing different measurements of *O. moschatus* postcranial elements from Cowshead Cave in comparison with modern specimens from Greenland, kept at the Natural History Museum of Denmark and (for metacarpals) with other Pleistocene fossil specimens from Eurasia: A, metacarpal: greatest length (GL)/width of the distal end (Wd); B, scapula: width of the glenoid cavity (WG)/greatest length of the Processus articularis (GLP); C, proximal phalanx: greatest length (GL)/width of the proximal end (Wp); D, distal phalanx: greatest length (GL)/greatest width (GW). Sources: 1, Bosscha Erdbrink (1983); 2, de Vries (1990); 3, Kerkhoff and Mol (1991); 4, Siegfried (1982); 5, Cregut-Bonnoure (2002); 6, Kahlke and Kahlke (1969); 7, own data D.A.-L. All measurements are in mm.

mm) is also greater than those of the two modern 18 months-old male skulls from Canada published by Allen (1913), which measure 355 and 360 mm.

The main skull sutures (between left and right frontals, between frontals and parietals and between parietals and occipitals) are still not fused, as they are in all the individuals of the same individual age of the modern population from Greenland.

6.1.4. Postcranial remains of the young individual

The postcranial elements of the young specimen are incompletely grown (Fig. 5h–k), evidenced by the lack of fusion at one or two of the epiphyses for each limb bone, and are noticeably smaller than the ones of the subadult individual. The distal humeral epiphysis is partially fused while the proximal one is unfused; the proximal radial epiphysis is almost totally fused but the distal one is unfused; both (proximal and distal) tibial epiphyses are totally unfused. This bone-development degree is the same as that observed in modern Greenland individuals aged 20 months old.

6.1.5. Date of death of the young individual

Overall, according to the teeth erupting and wearing degree, horn core development, cranial morphology and size, and bone fusion degree, we conclude that the young individual was a male of about 20 months of age.

In order to estimate the date of death, we must first consider the epoch of birth and, therefore, the calving period: musk ox calving takes place mainly from April to early June, possibly extending from late March until mid-June (Tener, 1965; Henrichsen and Grue, 1980). Consequently, the young specimen from Cowshead died most probably between December and February, i.e., in winter.

6.2. Subadult individual

Remains from the subadult specimen include only postcranial elements (Fig. 5a–g). These are well distinguishable from those of the young specimen because of their markedly larger size.

6.2.1. Postcranial remains of the subadult individual

The age of death of this individual can be estimated from the growing stage of each bone. Two of them are incompletely grown: the proximal radial epiphysis is totally fused but the distal one is still unfused; the proximal tibial epiphysis remains unfused while the distal one is completely fused. However, other elements like scapula, metacarpal, proximal phalanx and distal phalanx are fully grown. This same asynchrony in the fusion stage of different bones was also observed in five recent musk ox skeletons from Greenland aged between 38 and 44 months. In all of them, radii and tibias preserved one unfused epiphysis while metacarpals and phalanges were fully grown. In addition, a metacarpal from a skeleton of a 32 months-old individual retained an unfused distal epiphysis, which suggests that total fusion of the metacarpals probably occurs between 32 and 38 moths.

Although a more accurate estimation is not possible, comparison of the subadult individual from Cowshead with the recent skeletons from Greenland suggests that it died at about 38–44 months, that is, roughly in its fourth year of life.

The sexing of this individual cannot be accurately performed since none of the preserved elements show dimorphic features. However, the extremely large size of the elements (Section 5.4), which surpasses the size of the modern specimens from Greenland, suggests that it probably corresponds to a male.
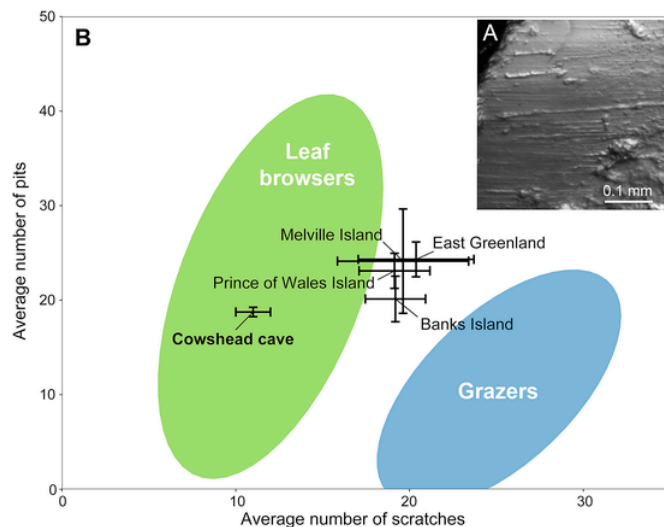

Fig. 12. A, photomicrograph of the tooth enamel surface on the left M^1 of *O. moschatus* from Cowshead cave (35 times magnification). B, bivariate plot of the average numbers of pits and scratches for the fossil *O. moschatus* from Cowshead cave compared to extant populations of muskox. Coloured areas correspond to the Gaussian confidence ellipses (p = 0.95) on the centroid for the extant leaf browsers and grazers from Solounias and Semprebon (2002).

7. Dietary traits of the Cowshead Cave musk ox inferred from microwear analysis

7.1. Results of the microwear analysis

The microscopic observation revealed that the enamel of the occlusal surface of CH-1 teeth is well preserved (Fig. 12A) and both left and right M^1 are suitable for the quantitative microwear analysis.

The low numbers of scratches and pits, as well as the presence of large pits and gouges, place this specimen among the extant leaf browsers (Table 4; Fig. 12A, B). The presence of hyper-coarse scratches and the high Scratch Width Score (SWS) suggest the consumption of woody parts of plants, such as bark or twigs (Semprebon et al., 2011). In the case of the musk ox, these microwear features were most probably produced by the twigs of small trees or shrubs. The absence of puncture pits allows discarding the consumption of fruits or seeds. The diet of this individual at the time of death was that of a typical browser, probably composed of leaves and twigs of trees or bushes.

In comparison, extant populations of musk ox have higher numbers of scratches and plot among the mixed feeders (Table 4; Fig. 12B). In all populations, the sample is averaging the signal of individuals dead at different seasons of the year (i.e. more browsing or more grazing) into a seasonal mixed feeding signal. The microwear pattern observed on the specimen from Cowshead Cave plots within the leaf browsers because it is a single individual and it reflects the diet at the time of death, browsing in that case.

7.2. Discussion of the dietary traits

The microwear pattern on the molars of the musk ox from Cowshead Cave suggests a browsing diet based on twigs and leaves at the time of death. The leaf browsing diet is consistent with the plant remains and microfossil recovered in Late Pleistocene musk ox teeth from the North Sea, where birch pollen was identified together with Asteraceae, Ericaceae and Poaceae (van Geel et al., 2019). Studies of the musk ox diet in extant populations report a high variability that reflects the diversity of habitats ranging from high polar desert to subarctic continental vegetation, but also seasonal changes mainly related to the availability of the resources. Generally, the musk ox is an adaptive forager that uses large amounts of plants with high-fibre content, usually dominated by graminoid plants when available (Klein, 1992). In the southern areas of the musk ox distribution, willows (in the form of shrubs) constitute a major part of its diet, when they are available (Tener, 1965). On Banks Island, willow and sedge represent most of the musk ox diet but their proportion varies seasonally (Larter and Nagy, 2004). Willow is an important part of the musk ox late winter diet. The decrease of the sedge proportion and the increase of willow in the musk ox diet from November to January on Banks Island are most likely caused by changes in forage availability (Larter and Nagy, 2004). More generally, graminoids, especially sedges (*Carex* sp.) play a major role in summer diets of musk ox (Tener, 1965; Wilkinson et al., 1976). Woody species are highly consumed at all seasons on

Table 4
Average numbers of pits (NP) and scratches (NS), scratch width score (SWS) and presence (pres.)/absence (abs.) of large pits or percentages of individuals with large pits (LP), gouges (G), cross scratches (XS), hyper-coarse scratches (HC), puncture pits (PP) for the 2 M of *Ovibos moschatus* from Cowshead Cave and from extant populations.

Locality (Tooth)		N	NP	NS	LP	G	SWS	XS	HC	PP
Cowshead Cave	(RM1)	–	18.5	10.5	pres.	pres.	2	abs.	pres.	abs.
	(LM1)	–	19.0	11.5	pres.	pres.	2	abs.	pres.	abs.
East Greenland		8	24.3	20.4	75%	25%	1.1	0	abs.	abs.
Banks Island		8	20.1	19.2	87.5%	75%	1	0	abs.	abs.
Melville Island		8	24.1	19.6	37.5%	37.5%	1.1	37.5	abs.	abs.
Prince of Wales Island		15	23.1	19.1	26.7%	26.7%	1.2	20	abs.	abs.

the mainland where musk ox populations occur within the limits of the boreal forest (Tener, 1965). In faecal samples from high Arctic sites, representing late winter and spring feeding, roughly 50% of identifiable fragments were woody fibres and over one-third were sedges. In the Taimyr Peninsula, musk ox depends on graminoids and willows in winter (Rapota, 1984). Consequently, the high amount of browse and woody parts in the diet of the young individual from Cowshead Cave would correspond to a winter diet. This conclusion is supported by the season of death estimated from tooth eruption and wear.

8. Paleobiogeographical implications

The occurrence of musk ox at Cowshead Cave (located at latitude 43.2°N and longitude 4.7°W) is of great paleobiogeographic significance since it represents the first occurrence of this cold-adapted ungulate in NW Iberia (Cantabrian Region) and, moreover, because it extends to the SW the known Eurasian distribution range of this species (Fig. 13).

O. moschatus is present in Europe probably since MIS 16 (at the site of Süßenborn, Germany; H.-D. Kahlke, 1963; R.-D. Kahlke, 2014) and reached its largest distribution range during the coldest episodes of the Late Pleistocene (MIS 5d - MIS 2; Kahlke, 2014). Detailed studies on the Pleistocene distribution of *O. moschatus* across Europe were carried out by Crégut-Bonnoure (1984), Kahlke (1999, 2014) and Raufuss and von Koenigswald (1999): its range spread through most of continental Europe reaching northern Iberia and the British Isles to the W, southern Scandinavia to the N, the Alps and Carpathians to the S and reaching the Urals to the E (Fig. 13). Eastward of the Urals, its distribution extended across northern Asia, covering W

and NE Siberia to the Liakhov and the New Siberian Islands, and is limited southwards by the arid areas of Central Eurasia (Kahlke, 1999, 2014). The southernmost finds come from the Arbreda and Can Rubau sites (Estévez Escalera, 1978; Álvarez-Lao and García, 2010), both in Gerona (NE Iberia), at latitude 42°N. The westernmost known boundary of the *Ovibos* Eurasian range corresponds to the site of Aghnadarragh, in Northern Ireland (Lister and Grün, 2015), at about longitude 6.2°W.

Markova et al. (2015) identified changes in the geographical distribution of *O. moschatus* in Eurasia related to the sequence of climatic changes, during the second part of the Late Pleistocene and the Holocene (MIS 3–1). They conclude that its greatest extension occurred during the geochronological intervals Denekamp and LGM (Last Glacial Maximum). The musk ox assemblage from Cowshead Cave (dated to 34.9 cal ka BP, see Section 9) corresponds to the Denekamp interval, which is consistent with the results of Markova et al. (2015) and delimits a more southern and western distribution boundary than that known for this episode.

The distribution of *O. moschatus* in the Iberian Peninsula is consistent with those of other cold-adapted taxa: all Iberian occurrences of reindeer (*Rangifer tarandus*) are also located in the Cantabrian Region and Northern Catalonia (Altuna, 1996; Álvarez-Lao and García, 2011a; Gómez-Olivencia et al., 2014; Álvarez-Lao et al., 2015), West and East of the Pyrenees, respectively, where existed topographically low areas which acted as corridors allowing the entrance of mammal faunas from continental Europe to the Iberian Peninsula (Álvarez-Lao and García, 2011a). Likewise, most of the Iberian occurrences of *Mammuthus primigenius* and *Coelodonta antiquitatis* are also located
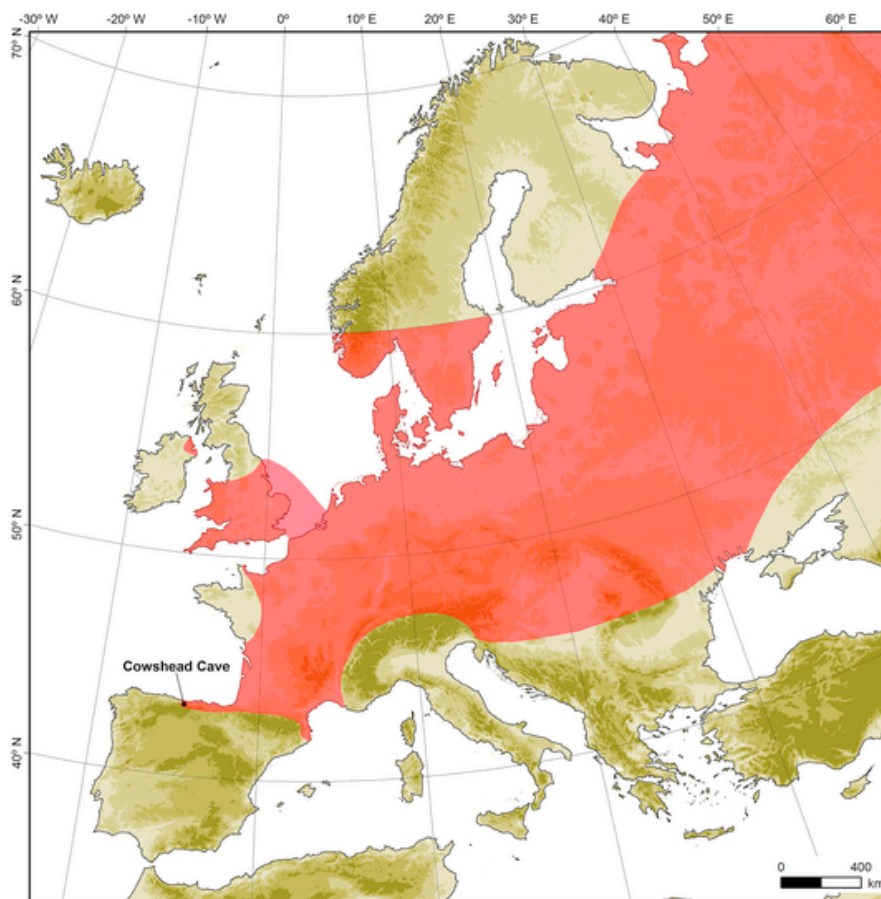

Fig. 13. Late Pleistocene maximum distribution of *Ovibos moschatus* in Europe (shaded in red) following Kahlke (2014) with additions after Lister and Grün (2015) and this work. (For interpretation of the references to colour in this figure legend, the reader is referred to the Web version of this article.)

at these same areas (Altuna, 1996; Álvarez-Lao and García, 2011b, 2012; Álvarez-Lao et al., 2017).

The finding of musk ox remains at Cowshead Cave, a location away from other sites where this species occurred, could suggest a possible southward winter migration from mainland Europe, which would involve a seasonal movement of more than 250 km. However, considering the migratory behaviour of modern musk ox populations, this possibility seems unlikely: in contrast to other ungulates such as reindeer, in which many populations perform long seasonal migrations between summer and winter ranges (Moen et al., 2006; Schmidt et al., 2016), most authors agree that musk ox is a relatively sedentary species which only makes short displacements between its winter and summer areas (Harington, 1961; Tener, 1965; Lent, 1988; Klein, 1992; Moen et al., 2006; Sheremetev et al., 2014; Schmidt et al., 2016). According to Tener (1965), these seasonal movements generally do not exceed 50 km, which is consistent with data recently obtained by GPS location of populations from NE Greenland (Schmidt et al., 2016). However, the possible migratory behaviour of Late Pleistocene musk ox populations is unknown. Following Siegfried (1982), the short, stocky and flattened metacarpal of *Ovibos moschatus* is indicative of a tundra inhabitant who behaves predominantly faithfully to the place without much movement. According to this assertion, we cannot reject the possibility that the longer and slender metacarpals of Late Pleistocene musk ox populations could be related to a more migratory behaviour.

From a topographical perspective, the location of Cowshead Cave at a high altitude (843 m a.s.l.) is consistent with the assumption that these animals (at least the young individual) died in winter. The musk ox is adapted to living in regions of low precipitation where winter snow cover is either shallow or irregularly distributed allowing the persistence of areas with accessible winter forage (Lent, 1988). Thus, while in summer the musk oxen frequent productive areas such as river valleys, lakeshores and meadows, in winter these lowland settings are covered by a thick layer of snow, preventing them from accessing the vegetation there and, thus, forcing them to move to wind-swept areas at higher elevations, wherever suitable forage exists and snow depth is kept low by prevailing winds (Tener, 1965; Stuart, 1982; Lent, 1988; Gustine et al., 2011; Schmidt et al., 2016; van Geel et al., 2019). Musk ox remains were found even at higher elevations than Cowshead Cave at other European sites: according to Raufuss and von Koenigswald (1999), the highest altitude localities yielding *Ovibos* remains are Schnurenloch cave (Switzerland, 1250 m a.s.l.) and Potocka cave (Slovenia, 1650 m a.s.l.).

9. Paleoenvironmental implications

The chronology of the *O. moschatus* assemblage from Cowshead Cave was determined by an AMS radiocarbon date of 34.9 ± 0.4 cal ka BP (D-AMS 029027) falling within MIS 3 (Fig. 14). The presence of musk ox at NW Iberia in this chronology is indicative of cold and arid environmental conditions, which is highly relevant from a paleoenvironmental perspective and is consistent with the paleontological record: this date corresponds to one of the episodes in which a greater number of cold-adapted mammal occurrences is registered in the Iberian Peninsula, especially from the Cantabrian Region (Fig. 14).

The chronology of Cowshead Cave overlaps with the age of the Urtiagako Leizea (Guipúzcoa) assemblage, at which reindeer is, by far, the dominant species (comprising 83.5% of the ungulates) and, moreover, woolly mammoth and woolly rhino also occur (Altuna, 1984; Altuna and Mariezkurrena, 2010), documenting one of the MIS 3's coldest episodes recognised in the Cantabrian Region. In addition, reindeer fossils were recovered at other sites from this region of coincident or similar age, such as La Garma, in Cantabria (Gómez-Olivencia et al., 2014), Arlanpe, in Vizcaya (Gómez-Olivencia et al., 2014) and Aitzbitarte III, in Guipúzcoa (Altuna and Mariezkurrena, 2011;

Marín-Arroyo et al., 2018); likewise, woolly rhinoceros occurred at the nearby cave of Jou Puerta, in Asturias (16 km N of Cowshead Cave), in the same time span (Álvarez-Lao, 2014). Moreover, the age of the Cowshead Cave musk ox corresponds to the episode at which the southernmost registered spread of woolly mammoth is documented in Europe (in Padul, southern Spain, Álvarez-Lao et al., 2009), contemporary with the development of an *Artemisia*-dominated steppe in Southern Iberia (Fernández et al., 2007).

Small-mammal remains are among the most paleoenvironmentally informative fossils; however, the micromammal record from Cowshead Cave resulted very poor: the only identifiable element is an arvicoline molar fragment (Fig. S2, Appendix A), whose size and shape in occlusal view match those of the T1 (first triangle, following the nomenclature of van der Meulen, 1973) of a vole M_3. Despite it being only a small fragment, it shows features of systematic significance: the morphology of the basal portion in lateral view is indicative of a rooted molar; the enamel thickness in the anterior wall of the prism (measurable in occlusal view) is greater than that of the posterior one. These two features are distinctive of *Pliomys coronensis* ($= P. lenki$). Although this extinct vole is not environmentally very informative, its occurrence at Cowshead Cave is interesting from a chronological perspective, since it is a common species in MIS 3 assemblages of the Cantabrian Region (Sesé, 2005), such as El Castillo (Sesé, 2017) and El Esquilleu (Uzquiano et al., 2012), mainly linked to rocky areas (Cuenca-Bescós et al., 2010).

From a paleoanthropological viewpoint, the Cowshead Cave assemblage is also coeval with the end of the Aurignacian technocomplex (34.6–33.1 cal ka BP) and the first Gravettian evidences (36.8–35 cal ka BP) at the Cantabrian Region (Marín-Arroyo et al., 2018). It would be of interest to consider the possible influence of the severe environmental conditions evidenced at that time in Cowshead Cave (and other sites above indicated), to discuss the likely scenario in which this cultural transition occurred.

10. Conclusions

The remarkable musk ox assemblage from Cowshead Cave is of great paleobiogeographic relevance since it involves the first occurrence of this species at NW Iberia (Cantabrian Region) and, moreover, because it represents the SW boundary of its Eurasian distribution range.

The fossil assemblage corresponds to at least two individuals: one young and one subadult. The bone accumulation was produced by accidental falling of the animals through a vertical shaft (of at least 13 m in depth). The lack of bone fragmentation by human or carnivore activity allowed an exceptional preservation of the fossils.

A detailed morphometric and morphologic study of the skull from the young individual (CH-1), in comparison to a sample of modern specimens of similar individual age from Greenland, showed morphometric and morphologic peculiarities:

-Morphometrically, the skull CH-1 resulted larger than the modern specimens of the comparison sample. Among the teeth, M^1 from CH-1 are also greater than almost all the comparison specimens.

-Morphologically, the skull is broader in front of the orbits (i.e. anteorbital constriction is very slight), giving it a particular triangular shape in the rostral area. This constriction is quite marked in the recent specimens from Greenland and, consequently, the rostral area is visibly more slender. In addition, postorbital constriction is noticeably more pronounced in CH-1 than in the modern specimens.

-Deciduous teeth also show interesting peculiarities: dP^4 show well-developed entostyles or median pillars, while entostyles are poorly developed or absent at all the studied recent dP^4 from Greenland. Furthermore, in dP_4 two pillars or ectostylids are well developed, which is a trait of special relevance since pillars do not occur at any of the revised recent dP_4 from Greenland.
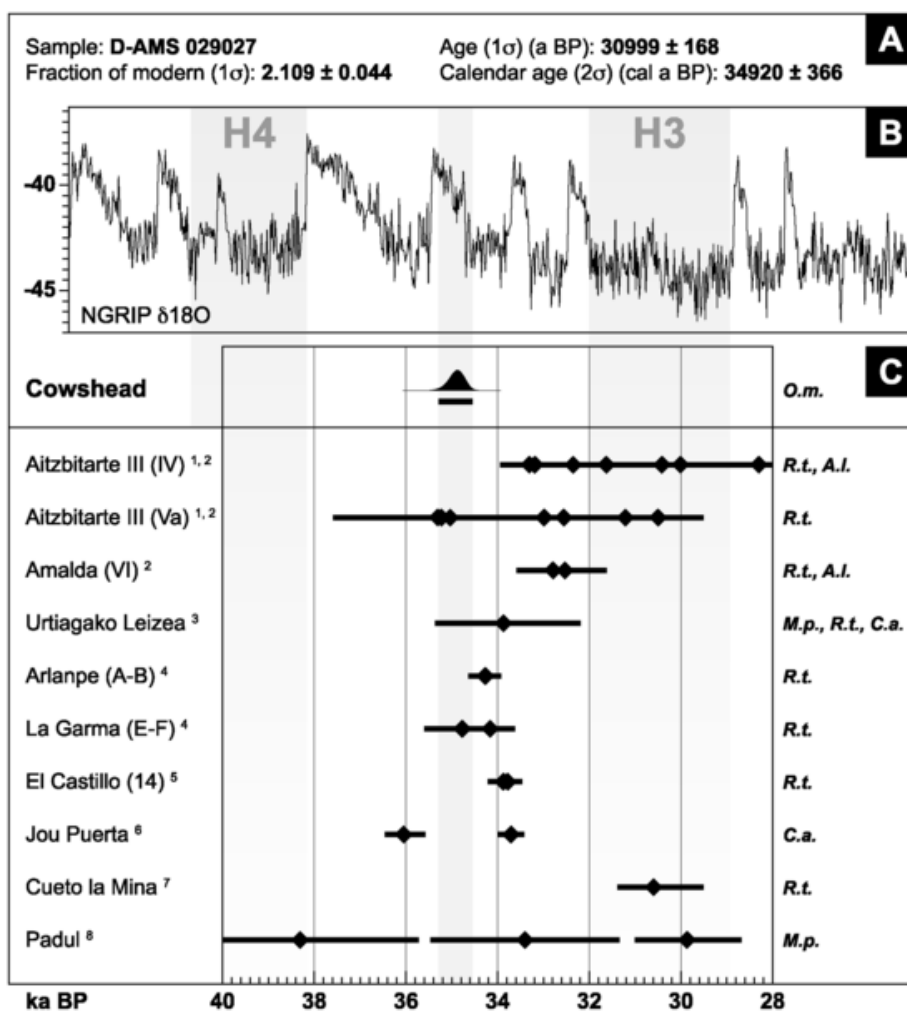
Fig. 14. A, radiocarbon date of the *O. moschatus* remains from Cowshead Cave. B, NGRIP paleoclimatic $\partial^{18}O$ curve (North GRIP Members, 2004). C, graphical expression of the date from Cowshead Cave compared to calibrated dates from other Iberian assemblages of similar age comprising cold-adapted mammal species (specified at the right). Abbreviations: H - Heinrich Event; *O.m.* - *Ovibos moschatus*; *R.t.* - *Rangifer tarandus*; *A.l.* - *Alopex lagopus*; *M.p.* - *Mammuthus primigenius*; *C.a.* - *Coelodonta antiquitatis*. Sources: 1, Altuna (2011); 2, Marín-Arroyo et al. (2018); 3, Altuna and Mariezkurrena (2010); 4, Gómez-Olivencia et al. (2014); 5, Bernaldo de Quirós Guidotti et al. (2012); 6, Álvarez-Lao (2014); 7, Hoyos and Rasilla (1994); 8, Álvarez-Lao et al. (2009).

The metacarpal of the subadult individual (CH-20) was compared to a sample of recent specimens from Greenland and to other Pleistocene fossil metacarpals from Europe and Siberia. Morphometrically, all the Pleistocene metacarpals are larger than the modern ones, with no overlap in length between both populations (specimen CH-20 is one of the largest of the entire sample). Morphologically, Pleistocene metacarpals (including CH-20) are remarkably more slender than all those from the modern sample. Other postcranial elements from Cowshead Cave (scapula and phalanges) resulted also larger than almost the entire modern sample from Greenland.

According to tooth eruption and wear degree, horn core development, cranial morphology and size, and bone fusion degree, we conclude that the young individual (including the skull CH-1) was a male of about 20 months of age. Consequently, the date of death can be estimated between December and February, i.e., in winter. This is consistent with the tooth microwear pattern, which suggests a winter diet, and with the location of the assemblage at a high altitude cave.

Bone fusion degree in the limb bones of the subadult individual suggests that it died at about 38–44 months, that is, roughly in its fourth year of life.

The occurrence of musk ox in Cowshead Cave evidences the development of cold and arid environmental conditions in mountain areas of NW Iberia at 34.9 ± 0.4 cal ka BP. Open landscapes most proba-

bly dominated during this time in the area; however, the existence of small trees or shrubs in the surroundings of Cowshead Cave is suggested by the predominantly browsing diet of the young individual inferred by its tooth microwear pattern. This cold and arid environment is consistent with the regional paleontological record, since a number of contemporary assemblages from the Cantabrian Region yielded remains of other species of the mammoth fauna, such as *R. tarandus*, *M. primigenius* and *C. antiquitatis*.

Declaration of competing interest

The authors declare that they have no known competing financial interests or personal relationships that could have appeared to influence the work reported in this paper.

Acknowledgements

cas de movilidad de excelencia para docentes e investigadores de la Universidad de Oviedo, 2019". For their kindness allowing access to the collections of the NHMD, our thanks are due to the curators Eline Lorenzen and Morten Tange Olsen. Thanks to Tresviso Cave Project for the cave data provided. For assistance in field work, thanks to Victoria Álvarez (Onís) and, especially, to Pablo Solares (Llanes) who also carried out a careful preparation of the fossils. For information, discussion and other support, thanks to Dick Mol (Hoofddorp), Ralf-D. Kahlke (Weimar), Adrian M. Lister (London), Alexei Tikhonov (St. Petersburg), Pablo Turrero (Oviedo), Mario Menéndez (Madrid) and Marcos Méndez (Madrid). We also thank the Administration and technical staff of the National Park of Picos de Europa for their interest and assistance, and especially to Miguel Menéndez de la Hoz. Special thanks to two anonymous reviewers who greatly helped to improve the manuscript.

Appendix A. Supplementary data

Supplementary data to this article can be found online at https://doi.org/10.1016/j.quascirev.2020.106336.

References

Allen, J A, 1913. Ontogenetic and other variations in muskoxen, with a systematic review of the muskox group, recent and extinct. Mem. Am. Musuem Nat. Hist. 1 (4), 103–226.

Alonso, V, 1998. Covadonga national park (western Massif of Picos de Europa, NW Spain): a calcareous deglaciated area. Trab. Geol. 20, 167–181.

Altuna, J, 1984. Primer hallazgo de Mamut (*Mammuthus primigenius* Blumenbach) en el País Vasco Meridional. Munibe 36, 27–32.

Altuna, J, 1996. Faunas de clima frío en la Península Ibérica durante el Pleistoceno Superior. In: Ramil-Rego, P, Fernández Rodríguez, C, Rodríguez Gutián, M (Eds.), Biogeografía Pleistocena-Holocena de la Península Ibérica. Xunta de Galicia, Santiago de Compostela, pp. 13–39.

Altuna, J, 2011. Aitzbitarte III situación. Descripción del valle y de la cueva. Historia de las excavaciones recientes. Descripción del relleno (zona de entrada). Dataciones de radiocarbono. In: Altuna, J, Mariezkurrena, K, Ríos, J (Eds.), Ocupaciones humanas en Aitzbitarte III (País Vasco) 33.600-18.400 BP (Zona de entrada a la cueva), 5. Ekob, Vitoria, pp. 23–38.

Altuna, J, Mariezkurrena, K, 2010. Tafocenosis en yacimientos del País Vasco con predominio de grandes carnívoros. Consideraciones sobre el yacimiento de Amalda. Actas de la 1a Reunión de Científicos sobre cubiles de hiena (y otros grandes carnívoros) en los yacimientos arqueológicos de la Península Ibérica. Zona Arqueológica 13, 214–228.

Altuna, J, Mariezkurrena, K, 2011. Estudio de los macromamíferos del yacimiento de Aitzbitarte III (excavación de la entrada). In: Altuna, J, Mariezkurrena, K, Ríos, J (Eds.), Ocupaciones humanas en Aitzbitarte III (País Vasco) 33.600-18.400 BP (Zona de entrada a la cueva), 5. Ekob, Vitoria, pp. 395–480.

Álvarez-Lao, D J, 2014. The Jou Puerta cave (Asturias, NW Spain): a MIS 3 large mammal assemblage with mixture of cold and temperate elements. Palaeogeogr. Palaeoclimatol. Palaeoecol. 393, 1–19.

Álvarez-Lao, D J, García, N, 2010. Chronological distribution of Pleistocene cold-adapted large mammal faunas in the Iberian Peninsula. Quat. Int. 212, 120–128.

Álvarez-Lao, D J, García, N, 2011. Geographical distribution of Pleistocene cold-adapted large mammal faunas in the Iberian Peninsula. Quat. Int. 233, 159–170.

Álvarez-Lao, D J, García, N, 2011. Southern dispersal and palaeoecological implications of woolly rhinoceros (*Coelodonta antiquitatis*): review of the Iberian occurrences. Quat. Sci. Rev. 30, 2002–2017.

Álvarez-Lao, D J, García, N, 2012. Comparative revision of the Iberian woolly mammoth (*Mammuthus primigenius*) record into a European context. Quat. Sci. Rev. 32, 64–74.

Álvarez-Lao, D J, Kahlke, R-D, García, N, Mol, D, 2009. The Padul mammoth finds – on the southernmost record of *Mammuthus primigenius* in Europe and its southern spread during the Late Pleistocene. Palaeogeogr. Palaeoclimatol. Palaeoecol. 278, 57–70.

Álvarez-Lao, D J, Ruiz-Zapata, M B, Gil-García, M J, Ballesteros, D, Jiménez-Sánchez, M, 2015. Palaeoenvironmental research at Rexidora Cave: new evidence of cold and dry conditions in NW Iberia during MIS 3. Quat. Int. 379, 35–46.

Álvarez-Lao, D J, Rivals, F, Sánchez-Hernández, C, Blasco, R, Rosell, J, 2017. Ungulates from teixoneres cave (Moià, Barcelona, Spain): presence of cold-adapted elements in NE Iberia during the MIS 3. Palaeogeogr. Palaeoclimatol. Palaeoecol. 466, 287–302.

Baena Preysler, J, Carrión Santafé, E, Torres Navas, C, Vaquero Rodríguez, M, 2019. Mousterian inside the upper paleolithic? The last interval of El Esquilleu (Cantabria, Spain) sequence. Quat. Int. 508, 153–163.

Ballesteros, D, Jiménez-Sánchez, M, Giralt, S, García-Sansegundo, J, Meléndez-Asensio, M, 2015. A multi-method approach for speleogenetic research on alpine karst caves. Torca La Texa shaft, Picos de Europa (Spain). Geomorphology 247, 35–54.

Ballesteros, D, Giralt, S, García-Sansegundo, J, Jiménez-Sánchez, M, 2019. Quaternary regional evolution based on karst cave geomorphology in Picos de Europa (Atlantic Margin of the Iberian Peninsula). Geomorphology 336, 133–151.

Barron, E, Pollard, D, 2002. High-resolution climate simulations of oxygen Isotope stage 3 in Europe. Quat. Res. 58, 296–309.

Bernaldo de Quirós Guidotti, F, Castaños Ugarte, P M, Maíllo Fernández, J M, Neira Campos, A N, 2012. El Gravetiense de la cueva de El Castillo: nuevos datos. In: Heras Martín, C de las, Lasheras Corruchaga, J A, Arrizabalaga Valbuena, A, Rasilla Vives,

M de la (Eds.), Pensando en el Gravetiense: nuevos datos para la región cantábrica en su contexto peninsular y pirenaico, 23. Monografías del Museo Nacional y Centro de Investigación de Altamira, pp. 264–325.

Bosscha Erdbrink, D P, 1983. More fossil material of *Ovibos* from the low countries and the north sea. Proc. Koninklijke Nederlandse Akademie van Wetenschappen, Ser. B 86 (1), 39–53.

Bronk Ramsey, C, 2017. Methods for summarizing radiocarbon datasets. Radiocarbon 59 (2), 1809–1833.

Campos, P F, Willerslev, E, Sher, A, Orlando, L, Axelsson, E, Tikhonov, A, Aaris-Sorensen, K, Greenwood, A D, Kahlke, R-D, Kosintsev, P, Krakhmalnaya, T, Kuznetsova, T, Lemey, P, MacPhee, R, Norris, C A, Shepherd, K, Suchard, M A, Zazula, G D, Shapiro, B, Gilbert, M T P, 2010. Ancient DNA analyses exclude humans as the driving force behind late Pleistocene musk ox (*Ovibos moschatus*) population dynamics. Proc. Natl. Acad. Sci. Unit. States Am. 107 (12), 5675–5680.

Crégut-Bonnoure, E, 1984. The Pleistocene Ovibovinae of Western Europe: tempospatial expansion and paleoecological implications. Biol. Pap. Univ. Alsk. Spec. Rep. 4, 136–144.

Crégut-Bonnoure, E, 2002. Les Ovibovini et Caprini (Mammalia, Artiodactyla, Bovidae, Caprinae) du Plio-Pléistocène d'Europe: systématique, évolution et biochronologie PhD Thesis. University Claude-Bernard, Lyon 1.

Cuenca-Bescós, G, Straus, L G, García-Pimienta, J C, González-Morales, M R, López-García, J M, 2010. Late quaternary small mammal turnover in the cantabrian region: the extinction of *Pliomys lenki* (Rodentia, Mammalia). Quat. Int. 212, 129–136.

de Vries, A J, 1990. *Ovibos moschatus* from the pleistocene of Dutch tidal flats (Wadden shallows). Cranium 7 (2), 78–82.

Estévez Escalera, J, 1978. Primer hallazgo del buey almizclado (*Ovibos moschatus*, Zimmermann) en el pleistoceno peninsular. Acta Geol. Hisp. 13, 59–60.

Ferguson, R S, 1991. Detection and classification of muskox habitat on Banks Island, northwest territories, Canada, using landsat thematic Mapper data. Arctic 44 (1), 66–74.

Fernández, S, Fuentes, N, Carrión, J S, González-Sampériz, P, Montoya, E, Gil, G, Vega-Toscano, G, Riquelme, J A, 2007. The Holocene and late pleistocene pollen sequence of carihuela cave, southern Spain. Geobios 40, 75–90.

Fernández-Gibert, E, Calaforra, J M, Rossi, C, 2000. Speleogenesis in the Picos de Europa Massif, northern Spain. In: Klimchouk, A, Ford, D, Palmer, A, Dreybrodt, W (Eds.), Speleogenesis: Evolution of Karst Aquifers. National Speleological Society, Huntsville, Alabama, pp. 352–357.

Flueck, W T, Smith-Flueck, J M, 2011. Intraspecific phenotypic variation in deer: the role of genetic and epigenetic processes. Anim. Prod. Sci. 51, 365–374.

García, N, Arsuaga, J L, 2003. Last glaciation cold-adapted faunas in the Iberian Peninsula. In: Reumer, J W F, De Vos, J, Mol, D (Eds.), Advances in Mammoth Research (Proceedings of the Second International Mammoth Conference, Rotterdam, May 16-20, 1999), 9. DEINSEA, pp. 159–169.

Gómez-Olivencia, A, Arceredillo, D, Álvarez-Lao, D J, Garate, D, San Pedro, Z, Castaños, P, Rios-Garaizar, J, 2014. New evidence for the presence of reindeer (*Rangifer tarandus*) on the Iberian Peninsula in the Pleistocene: an archaeopalaeontological and chronological reassessment. Boreas 43, 286–308.

Gustine, D D, Barboza, P S, Lawler, J P, Arthur, S M, Shults, B S, Persons, K, Adams, L G, 2011. Characteristics of foraging sites and protein status in wintering muskoxen: insights from isotopes of nitrogen. Oikos 120, 1546–1556.

Guthrie, R D, 1982. Mammals of the mammoth steppe as paleoenviromental indicators. In: Hopkins, D M, Matthews, J V, Schweger, C E, Young, S B (Eds.), Paleoecology of Beringia. Academic Press, New York, pp. 307–326.

Harington, C R, 1961. History, Distribution and Ecology of the Muskoxen MS Thesis. McGill University, Montreal.

Henrichsen, P, Grue, H, 1980. Age criteria in the muskox (*Ovibos moschatus*) from Greenland. Dan. Rev. Game Biol. 11 (4), 3–18.

Hoyos, M, Rasilla, M de la, 1994. Dataciones C14 del Paleolítico superior del abrigo de Cueto de la Mina (Posada de Llanes, Asturias). Trab. Prehist. 51 (2), 143–147.

Jiménez-Sánchez, M, Rodríguez-Rodríguez, L, García-Ruiz, J M, Domínguez-Cuesta, M J, Farias, P, Valero-Garcés, B, Moreno, A, Rico, M, Valcárcel, M, 2013. A review of glacial geomorphology and chronology in northern Spain: timing and regional variability during the last glacial cycle. Geomorphology 196, 50–64.

Kahlke, H-D, 1963. *Ovibos* aus den Kiesen von Süßenborn. Ein Beitrag zur Systematik und Phylogenie der Ovibovini und zur Stratigraphie des Pleistozäns. Geologie 12, 942–972.

Kahlke, H-D, 1969. Die *Ovibos*-Reste aus den Kiesen von Süßenborn bei Weimar. Paläont. Abh. A III (3–4), 521–529.

Kahlke, R-D, 1999. The History of the Origin, Evolution and Dispersal of the Late Pleistocene Mammuthus-Coelodonta Faunal Complex in Eurasia (Large Mammals). Fenske Companies, Rapid City.

Kahlke, R-D, 2014. The origin of Eurasian mammoth faunas (*Mammuthus-Coelodonta* faunal complex). Quat. Sci. Rev. 96, 32–49.

Kerkhoff, N, Mol, D, 1991. Inventarisatie van Nederlandse vondsten van de muskusos, *Ovibos moschatus* (Zimmermann, 1780). Cranium 8 (2), 65–70.

Khan, E, 1966. *Ovibus pallantis rhenanus* nov. subsp., an extinct *Ovibos* of Weinheim, Rhine Valley, Germany. Mittl. Bayer. Staatssamml. Palaontol. Hist. Geol. 6, 133–142.

Klein, D R, 1964. Range-related differences in growth of deer reflected in skeletal ratios. J. Mammal. 45, 226–235.

Klein, D R, 1992. Comparative ecological and behavioral adaptations of *Ovibos moschatus* and *Rangifer tarandus*. Rangifer 12, 47–55.

Klein, D R, Meldgaard, M, Fancy, S G, 1987. Factors determining leg length in *Rangifer tarandus*. J. Mammal. 68, 642–655.

Kuzyk, G W, Dehn, M M, Farnell, R S, 1999. Body-size comparisons of alpine- and forest-wintering woodland caribou herds in the Yukon. Can. J. Zool. 77, 1017–1024.

Larter, N C, Nagy, J A, 2004. Seasonal changes in the composition of the diets of Peary caribou and muskoxen on Banks Island. Polar Res. 23, 131–140.

Lent, P C, 1988. Ovibos moschatus. Mamm. Species 302, 1–9.

Lister, A M, Grün, R, 2015. Mammoth and musk ox ESR-dated to the early Midlandian at Aghnadarragh, county Antrim, northern Ireland, and the age of the Fermanagh stadial. Geol. J. 50, 306–320.

Lönnberg, E, 1900. On the structure and anatomy of the musk-ox (*Ovibos moschatus*). In: Proceedings of the Zoological Society of London 1900. pp. 686–718.

Lorenzen, E D, Nogués-Bravo, D, Orlando, L, Weinstock, J, Binladen, J, Marske, K A, Ugan, A, Borregaard, M K, Gilbert, M T P, Nielsen, R, Ho, S Y W, Goebel, T, Graf, K E, Byers, D, Stenderup, J T, Rasmussen, M, Campos, P F, Leonard, J A, Koepfli, K-P, Froese, D, Zazula, G, Stafford, T W, Jr., Aaris-Sørensen, K, Batra, P, Haywood, A M, Singarayer, J S, Valdes, P J, Boeskorov, G, Burns, J A, Davydov, S P, Haile, J, Jenkins, D L, Kosintsev, P, Kuznetsova, T, Lai, X, Martin, L D, McDonald, H G, Mol, D, Meldgaard, M, Munch, K, Stephan, E, Sablin, M, Sommer, R S, Sipko, T, Scott, E, Suchard, M A, Tikhonov, A, Willerslev, R, Wayne, R K, Cooper, A, Hofreiter, M, Sher, A, Shapiro, B, Rahbek, C, Willerslev, E, 2011. Species-specific responses of late Quaternary megafauna to climate and humans. Nature 479, 359–364.

MacPhee, R, Tikhonov, A, Mol, D, Greenwood, A, 2005. Late Quaternary loss of genetic diversity in muskox (*Ovibos*). BMC Evol. Biol. 5, 49.

Marín-Arroyo, A B, Ríos-Garaizar, J, Straus, L G, Jones, J R, Rasilla, M de la, González-Morales, M R, Richards, M, Altuna, J, Mariezkurrena, K, Ocio, D, 2018. Chronological reassessment of the middle to upper paleolithic transition and early upper paleolithic cultures in cantabrian Spain. PloS One 13 (4), e0194708.

Markova, A K, Puzachenko, A Y, van Kolfschoten, T, Kosintsev, P A, Kuznetsova, T V, Tikhonov, A N, Bachura, O P, Ponomarev, D V, van der Plicht, J, Kuitems, M, 2015. Changes in the Eurasian distribution of the musk ox (*Ovibos moschatus*) and the extinct bison (*Bison priscus*) during the last 50 ka BP. Quat. Int. 378, 99–110.

McLennan, S M, 2001. Relationships between the trace element composition of sedimentary rocks and upper continental crust. Geochem. Geophys. Geosyst. 2 Paper number 2000GC000109.

McMahon, T A, 1975. Allometry and biomechanics: limbbones in adult ungulates. Am. Nat. 109, 547–563.

Merino-Tomé, O, Suárez Rodríguez, A, Alonso, J, González Menéndez, L, Heredia, N, Marcos, A, 2013. Mapa Geológico Digital continuo E. 1:50.000, Principado de Asturias (Zonas: 1100-1000-1600). GEODE. Mapa Geológico Digital Continuo de España. SIGECO-IGME. http://cuarzo.igme.es/sigeco/default.htm.

Moen, J, Andersen, R, Illius, A, 2006. Living in a seasonal environment. In: Danell, K, Bergström, R, Duncan, P, Pastor, J (Eds.), Large Herbivore Ecology, Ecosystem Dynamics and Conservation. Cambridge University Press, pp. 50–70.

Mol, D, Zijlstra, L, 1994. Muskusossen uit de Nederlandse bodem. Grondboor Hamer 1, 8–16.

Moreno, A, Valero-Garcés, B L, Jiménez-Sánchez, M, Domínguez-Cuesta, M J, Mata, M P, Navas, A, González-Sampériz, P, Stoll, H, Farias, P, Morellón, M, Corella, J P, Rico, M, 2010. The last deglaciation in the Picos de Europa national Park (cantabrian mountains, northern Spain). J. Quat. Sci. 25 (7), 1076–1091.

Newman, G, Walker, J, 1987. Agua'86. Caves and Caving 36, 15–17.

Nieminen, M, Helle, T, 1980. Variations in body measurements of wild and semidomestic reindeer (*Rangifer tarandus*) in Fennoscandia. Ann. Zool. Fenn. 17, 275–283.

Putman, R, Flueck, W T, 2011. Intraspecific variation in biology and ecology of deer: magnitude and causation. Anim. Prod. Sci. 51, 277–291.

Rapota, V V, 1984. Feeding ecology of the Taimyr muskoxen. Biol. Pap. Univ. Alsk. Spec. Rep. 4, 75–80.

Raufuss, I, von Koenigswald, W, 1999. New remains of Pleistocene *Ovibos moschatus* from Germany and its geographic and stratigraphic occurrence in Europe. Geol. Mijnbouw 78, 383–394.

Reimer, P J, Bard, E, Bayliss, A, Beck, J W, Blackwell, P G, Bronk Ramsey, C, Buck, C E, Cheng, H, Edwards, R L, Friedrich, M, Grootes, P M, Guilderson, T P, Haflidason, H, Hajdas, I, Hatté, C, Heaton, T J, Hoffmann, D L, Hogg, A G, Hughen, K A, Kaiser, K F, Kromer, B, Manning, S W, Niu, M, Reimer, R W, Richards, D A, Scott, E M, Southon, J R, Staff, R A, Turney, C S M, van der Plicht, J, 2013. IntCal13 and Marine13 radiocarbon age calibration curves 0–50.000 years cal BP. Radiocarbon 55, 1869–1887.

Rodríguez-Rodríguez, L, Jiménez-Sánchez, M, Domínguez-Cuesta, M J, Aranburu, A, 2014. Research history on glacial geomorphology and geochronology of the Cantabrian Mountains, north Iberia (43–42°N/7–2°W). Quat. Int. 364, 6–21.

Ruiz-Fernández, J, Oliva, M, Cruces, A, Lopes, V, Freitas, M da C, Andrade, C, García-Hernández, C, López-Sáez, J A, Geraldes, M, 2016. Environmental evolution in the Picos de Europa (cantabrian mountains, SW Europe) since the last glaciation. Quat. Sci. Rev. 138, 87–104.

Schmidt, N M, van Beest, F M, Mosbacher, J B, Stelvig, M, Hansen, L H, Nabe-Nielsen, J, Grøndahl, C, 2016. Ungulate movement in an extreme seasonal environment: year-round movement patterns of high-arctic muskoxen. Wildl. Biol. 22, 253–267.

Semprebon, G, Sise, P, Coombs, M, 2011. Potential bark and fruit browsing as revealed by stereomicrowear analysis of the peculiar clawed herbivores known as chalicotheres (Perissodactyla, Chalicotherioidea). J. Mamm. Evol. 18, 33–55.

Serrano, E, González-Trueba, J J, González-García, M, 2012. Mountain glaciation and paleoclimate reconstruction in the Picos de Europa (Iberian Peninsula, SW Europe). Quat. Res. 78, 303–314.

Serrano, E, Gonzalez-Trueba, J J, Pellitero, R, Gomez-Lende, M, 2017. Quaternary glacial history of the Cantabrian Mountains of northern Spain: a new synthesis. In: Hughes, P D, Woodward, J C (Eds.), Special Publications, 433: Quaternary Glaciation in the Mediterranean Mountains. Geological Society of London, London, pp. 55–85.

Sesé, C, 2005. Aportación de los micromamíferos al conocimiento paleoambiental del Pleistoceno Superior de la Región Cantábrica: nuevos datos y síntesis. In: Montes Barquín, R, Lasheras Corruchaga, J A (Eds.), Neandertales Cantábricos, estado de la cuestión, 20. Monografías del Museo Nacional y Centro de Investigación de Altamira, pp. 167–200.

Sesé, C, 2017. Los micromamíferos (Eulipotyphla, Chiroptera, Rodentia y Lagomorpha) del yacimiento del Pleistoceno Superior de la cueva de El Castillo (Cantabria). Estud. Geol. 73 (2), e072.

Sher, A V, 1971. Mammals and Stratigraphy of the Pleistocene of the Extreme Northeast of the USSR and North America. Nauka Press, Moscow.

Sheremetev, I S, Rozenfeld, S B, Sipko, T P, Gruzdev, A R, 2014. Extinction of large herbivore mammals: niche characteristics of the musk ox *Ovibos moschatus* and the reindeer *Rangifer tarandus* coexisting in Isolation. Biol. Bull. Rev. 4 (5), 433–442.

Siegfried, P, 1982. Skeletteile des pleistozäinen Moschusochsen aus Westfalen. Paläontol. Z. 56, 125–130.

Smart, P L, 1984. The geology, geomorphology and speleogenesis in the eastern massifs, Picos de Europa, Spain. Cave Sci. 11, 238–245.

Smart, P L, 1986. Origin and development of glacio-karst closed depressions in the Picos de Europa, Spain. Z. Geomorphol. 30, 423–443.

Soergel, W, 1941. Der Moschusochse aus den altdiluvialen Kiesen von Süßenborn. – Beiträge zur Geologie von Thüringen 6, 138–149.

Solounias, N, Semprebon, G, 2002. Advances in the reconstruction of ungulate ecomorphology with application to early fossil equids. Am. Mus. Novit. 3366, 1–49.

Stefaniak, K, Lipecki, G, Nadachowski, A, Semba, A, Ratajczak, U, Kotowski, A, Roblíčková, M, Wojtal, P, Shpansky, A V, Malikov, D G, Krakhmalnaya, T V, Kovalchuk, O M, Boeskorov, G G, Nikolskiy, P A, Baryshnikov, G, Ridush, B, Jakubowski, G, Pawłowska, K, Cyrek, K, Sudoł-Procyk, M, Czyżewski, Ł, Krajcarz, M, Krajcarz, M T, Żeromska, A, Gagat, P, Mackiewicz, P, 2019. Diversity of muskox *Ovibos moschatus* (Zimmerman, 1780) (Bovidae, Mammalia) in time and space based on cranial morphometry. Hist. Biol.. doi:10.1080/08912963.2019.1666374.

Stuart, A J, 1982. Pleistocene Vertebrates in the British Isles. Longman.

Tener, J S, 1965. Muskoxen in Canada. A Biological and Taxonomic Review. Canadian Wildlife Service.

Tikhonov, A N, 1998. The finds of muskox (*Ovibos*) on the territory of the former USSR. In: Saunders, J J, Styles, B W, Baryshnikov, G F (Eds.), Quaternary Paleozoology in the Northern Hemisphere. Illinois State Museum Scientific Papers. pp. 341–356.

Uzquiano, P, Yravedra, J, Ruiz Zapata, B, Gil Garcia, M J, Sesé, C, Baena, J, 2012. Human behaviour and adaptations to MIS 3 environmental trends (>53–30 ka BP) at Esquilleu cave (Cantabria, northern Spain). Quat. Int. 252, 82–89.

van Andel, T H, 2002. The climate and landscape of the middle part of the Weichselian glaciation in Europe: the stage 3 project. Quat. Res. 57, 2–8.

van der Meulen, A J, 1973. Middle pleistocene smaller mammals from the Monte Peglia (orvieto, Italy) with special reference to the phylogeny of Microtus (Arvicolidae, Rodentia). Quaternaria 17, 1–144.

van Geel, B, Langeveld, B W, Mol, D, van der Knaap, P W O, van Leeuwen, J F N, 2019. Pollen and spores from molar folds reflect food choice of late Pleistocene and Early Holocene herbivores in The Netherlands and the adjacent North Sea area. Quat. Sci. Rev. 225, 106030.

Vereschagin, N K, Baryshnikov, G F, 1982. Paleoecology of the mammoth fauna in the Eurasian arctic. In: Hopkins, D M, Matthews, J V, Schweger, C E, Young, S B (Eds.), Paleoecology of Beringia. Academic Press, New York, pp. 267–279.

Von den Driesch, A, 1976. A guide to measurement of animal bones from archaeological sites. Peabody Museum Bull. 1, 1–137.

Wilkinson, P F, Shank, C C, Penner, D E, 1976. Muskox-caribou summer range on Banks Island, N.W.T. J. Wildl. Manag. 40, 151–162.